Adaptive Backstepping Based Control of Heave-Induced Pressure Deviations In Managed Pressure Drilling (MPD)

By
Atif Naveed
NUST201463951MSEECS61214F

Supervisor
Dr. Iftikhar Ahmad
Department of Electrical Engineering

A thesis submitted in partial fulfillment of the requirements for the degree of Masters of Science in Electrical Engineering (MS EE)

In
School of Electrical Engineering and Computer Science,
National University of Sciences and Technology (NUST),
Islamabad, Pakistan.

(January 2017)

Approval

It is certified that the contents and form of the thesis entitled "**Adaptive Backstepping Based Control of Heave-Induced Pressure Deviations In Managed Pressure Drilling (MPD)**" submitted by **Atif Naveed** have been found satisfactory for the requirement of the degree.

Advisor: **Dr. Iftikhar Ahmad**
Signature: ____________________

Date: ____________________

Committee Member 1: **Dr. Hammad Sherazi**

Signature: ____________________
Date: ____________________

Committee Member 2: **Dr. Ammar Hassan**

Signature: ____________________
Date: ____________________

Committee Member 3: **Miss. Neelma Naaz**

Signature: ____________________
Date: ____________________

Abstract

Managed pressure drilling (MPD) is a controlled process of offshore hydrocarbons' exploration. It is not only capable to handle weather's severe effects on drilling process but it also improves the efficiency of offshore drilling operations.

In drilling operation, circulating drilling fluid (with particular density to maintain desired pressure in the well) is pumped in drill-string through choke valve, and it leaves through the drill bit, cools and lubricates the bit and the drill-string, and shifts the drilled cuttings to the surface.
Besides this normal operation, heave motions force drill-string to move it vertically which introduce pressure deviations in mud pressure. These pressure fluctuation may damage the well. To vanish the effect of heave motion, a controller is required to control choke valve in such a way which regulate desired mud pressure in the well, throughout the operation.

In this thesis, two nonlinear controllers have been presented for verified two volumes model of well pressure dynamics. Backstepping controller controls the choke valve to suppress pressure fluctuation effectively, in the well. On the other hand, Adaptive backstepping controller guarantee to regulate pressure close to desired level irrespective of variation in one of system parameter. In the last, a table for performance analysis of proposed controllers has been presented.

Dedication

I dedicate this thesis to my parents; it was impossible for me to complete my thesis work without their love, supports and guidance.

Certificate of Originality

I hereby declare that this submission is my own work and to the best of my knowledge it contains no materials previously published or written by another person, nor material which to a substantial extent has been accepted for the award of any degree or diploma at NUST SEECS or at any other educational institute, except where due acknowledgement has been made in the thesis. Any contribution made to the research by others, with whom I have worked at NUST SEECS or elsewhere, is explicitly acknowledged in the thesis.

I also declare that the intellectual content of this thesis is the product of my own work, except for the assistance from others in the project's design and conception or in style, presentation and linguistics which has been acknowledged.

Author Name: **Atif Naveed**
Signature: ________________

Acknowledgment

First of all, I want to mention unconditional love and support of my parents, throughout my life. Thank you so much for giving me strength and belief to accomplish my dreams.

To my one and only brother, Mr. Saqib Naveed, I want to thank you from the bottom of my heart for your commendable guidance and support at every moment of crisis. Thank you very much for being more than loyal and caring to me.

To all my friends, thank you very much for your care, love and support, particularly during my thesis phase. Especially, Mr. Wasim Abbas, thank you so much for your caring attitude while sharing the same room for three months. Without your generous friendship in depressed situation, it was near to impossible for me to complete this thesis.

Sincere appreciation and acknowledgment are due to the following person for their guidance and assistance in the accomplishment of this study. To Dr. Iftikhar Ahmad Rana, my thesis supervisor, for his competent direction and support.

Table of Contents

List of Figures

List of Tables

Chapter 1

Introduction

1.1 Background and Motivation

In the mid 20^{th} century, very few people believed about the availability of hydrocarbon in north sea. But gas field found in Groningen, in 1959, diverted people attention towards north sea; some specialists started speculating it for oil in Norwegian sea. In 1962, irrespective of Norwegian geologist's disbelief about the presence of hydrocarbon in this sea, Phillips petroleum requested permission from Norwegian government for oil exploration on the Norwegian shelf, with offer of $16,0000$ USD, a month. This deal was declined by Norwegian government, but later in 1965, deal was made with Great Britain and Denmark about sharing the north sea. First Norwegian exploration well was drilled in 1966, which was unfortunately empty. Three years later, in 1969, Phillips petroleum found oil which was about to 320 km, south west of Stavanger. It added prominent rise in revenue of Norwegian government and motivated them for further exploration. Drilling operation had technological issues including weather and depth of well. As a result, it diverted researchers effort towards the exploration of hydrocarbon [2].

Coming towards present situation, as per the International Energy Agency report in [3], energy demand of the world will be increased about 44 percent from 2006 to 2030. Additionally, petroleum industry has many technical issues, because easily-attained petroleum reservoirs already exploited. Currently, reservoirs to be drilled are complex to drill, due to narrow pressure margin, and higher depth.

Drilling process is expensive as it includes drilling rig and crew during the drilling operation. To minimize drilling cost, an efficient and fast drilling system is needed. Highly-experienced driller are required to ensure fast and safe drilling operations; they should also have ability to tackle upsets while drilling. As this procedure includes communication between heavy-mechanical machinery with the possibilities of severe problems. The dangerous blowout of drill rig named as, Deepwater Horizon, in the Gulf of Mexico, in April 2010, see Figure 1.1, diverted the attention of researcher towards safety as well, in the field of exploration of hydrocarbon.

With reference to all discussed requirement, an drilling precess is required to drill successfully complex wells with increase demand of pressure control, cost-effectiveness and safety.

Figure 1.1: The drill rig blowout. (Photo: U.S. Coast Guard.)

1.2 Pressure Control

The process of oil well drilling, schematically illustrated in Figure 1.2, it consists boring a hole several kilometers deep into the ground, until a reservoir is reached. The hole is created by rotating a *drill bit* to which a downward force is applied [4]. The force, and in most cases the rotation, is applied by *drill string*, which transfers it to the bit. The drilling rig can be located on onshore or on an offshore platform, then either as a rig fixed on the sea bed or as floating a drilling ship.

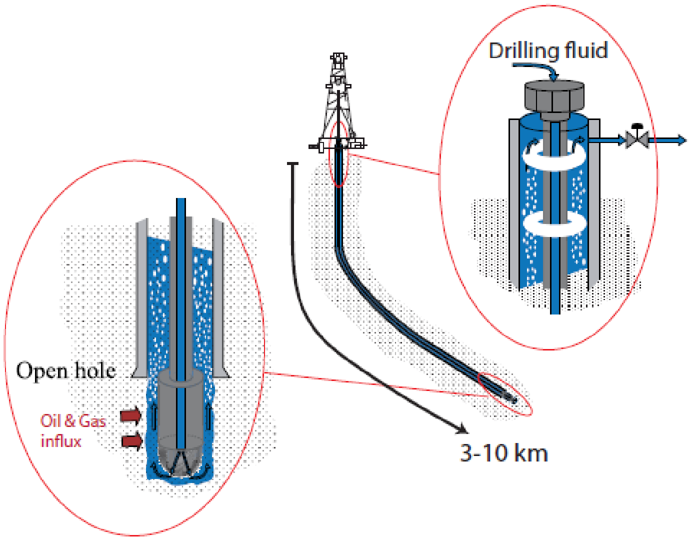

Figure 1.2: Schematic of well being drilled [1].

In drilling operation, *mud* is pumped in drill string, and it exits through the drill bit, cools and lubricates the bit and the drill string, and shifts the drilled cuttings to the surface. One of the main objective of drilling mud is to exert hydrostatic pressure, added to the frictional pressure drop in the annular space between the drill-string and wellbore/casing. Infect, it is required to balance the reservoir formation pressure. Consequently, the point where wellbore pressure equals the reservoir pore pressure is referred to as the *balance point*, and when the pressure in the wellbore exceeds and is less than the reservoir pressure, the well is said to be overbalanced and underbalanced, respectively.

As drilling progresses, casing is set at preplanned intervals to isolate the wellbore from the surrounding formation. The casing is a steel cylinder which is hammered into wellbore and cemented in it. The section of the well that has been drilled since the last casing was set, is susceptible to pressure changes in the wellbore and is called the *exposed zone*. Controlling pressure in the exposed zone is a major challenge in drilling.

1.2.1 Conventional drilling

Wellbore should be overbalanced, in conventional drilling, to avoid formation-fluid influx or hydrocarbons to the well. However, if wellbore pressure is too high, it could be higher than fracture pressure, resulting in rock breakdown and loss of drilling fluid to the formation. It could be costly because of potential damage of reservoir, high price of the lost fluid, and may in some cases prevent drilling from proceeding altogether. Therefore, in overbalanced drilling, well bore pressure should be higher than pore and collapse pressures of formation and lower than fracture pressure in the exposed zone, see Figure 1.3.

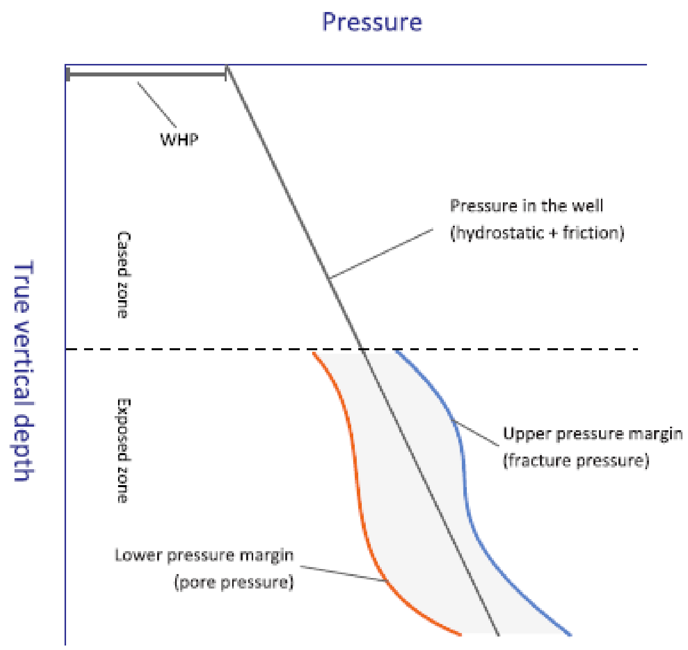

Figure 1.3: Distributed pressure margins for overbalanced drilling [1].

That is, we can write the pressure $P(x)$, at position x in the well, as

$$P(x) = P_{atm} + F_{ric}(x,t) + G_{rav}(x) \tag{1.1}$$

Where,

The wellhead pressure is atmospheric pressure, $WHP = P_{atm}$. However, Pressure profile throughout the wellbore can be controlled by circulating a new mud having different density, it modify the $G_{rav}(x)$ term in Equation 1.1. This $P(x)$ pressure have to be within pressure limits, according to pore and fracture pressure, respectively.

$$P_{pore}(x) < P(x,t) < P_{frac}(x), \tag{1.2}$$

For convenience, pressure in the exposed zone is usually lumped to a single point and referred to as the *bottom hole* pressure (BHP).

1.2.2 Managed pressure drilling

In narrow pressure margin wells such as deep-water offshore wells, formation and fracture pressures are very close. Managing the annular pressure is challenging and plays a vital role in successful drilling of these wells. Managed Pressure Drilling (MPD) techniques was introduced to control wellbore pressure having narrow pressure margins. It can be seen in [5]. MPD differs from conventional drilling as it includes rotating control device (RCD), see Figure 1.4, it is used to create a seal around the drill-string at the wellhead, which together with a $back-pressure\ choke$, enables manipulating the WHP. It, sometimes, coupled with a dedicated back-pressure pump to enable control when the main pump is shut off.

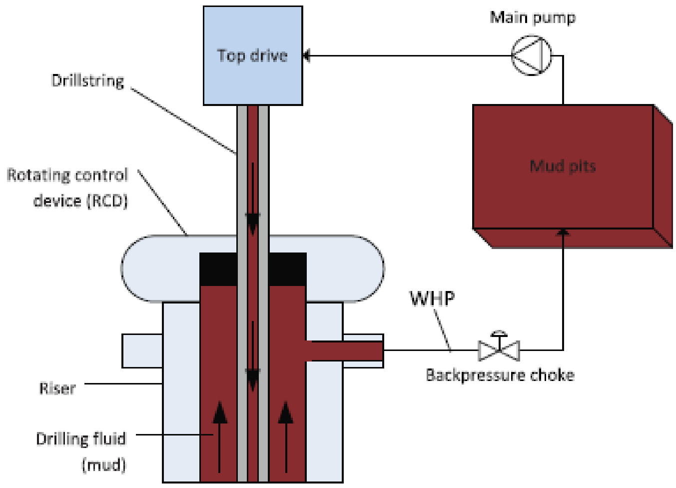

Figure 1.4: Topside part of a the closed circulation MPD system [1].

Apart from key advantage of MPD to ensure the drilling of wells where pressure margins are too narrow. It is also often used to handle uncertainty of the reservoir. This is primarily due to the improved well control capabilities offered by MPD [6], [7].

For managed pressure drilling, we have:

$$P(x) = WHP(t) + F_{ric}(x,t) + G_{rav}(x), \tag{1.3}$$

Where,

WHP can be effectively controlled by manipulating the opening of the back pressure choke.

In last decade, a commendable research has been devoted to managed pressure drilling internationally. Recently, control engineers are trying different control strategies to control the bottom hole pressure, in the oil industry. In [8], they used managed pressure to cement a seven inch liner on the Gullfaks field, is one of early example of MPD. Or more resent development in [9], where some requirements for high-performance control where presented.

In [10], using 3^{rd} order dynamical model, author followed Lyapunov approach to adopt unknown density and friction. Same third-order model and observer was used along with nonlinear control techniques to stabilize pressure of bottom hole, in [11] and [12].

An adaptive observer together with feedback controller was designed to tackle gas kick, in [13]. And, another nonlinear controller with verification of results by experiments, using full-scale drilling rig, was developed in [14].

The master thesis [15], is exploring the use of non-linear model predictive control with a combination of measurements and estimation for acquiring readings of the states. Where the bottom hole pressure is the controlled variable and the choke vale the manipulated variable.

1.2.3 MPD with heave motion

Managed pressure drilling control systems should also be able to tackle operational uncertainties, and disturbance along with requirement of narrow margin pressure drilling application. Disturbance available in real-time process, affects the system performance. Specific such one example is variation in pressure, while extending the drill string in order to drill more deeper in the well. During this pipe connection, the drill string is fixed to the drill floor which makes traditional heave compensation system unworkable. As a result, floating rig moves vertically with see waves, known as heave motion. As the drill string is clamped to the drill floor, this motion will pass into a drill bit which acts similar to a piston on the mud, in the well. Consequently, severe pressure fluctuation can be observed at the bottom of well. These fluctuations have been observed to have a magnitude higher than the standard limits for pressure regulation accuracy in MPD, which is about 2.5 bar [16].

Pressure increases when drill bit moves down into the well, this phenomena called surging. On the other hand, if drill bit moves upward, decreases the pressure (swabbing). Swabbing and surging pressures damages formation of well, neighbouring wells, and drilling equipments as specified in last section.

In the article [17], a semilinear dynamical model was created to capture the main dynamics of a MPD system, in the presence of heave disturbance, in a well, from the Ulrig test drilling facility, with a length of approximately 2000 m with water based mud. This model contained nine ordinary differential equations, and a choke equation. They also presented two controllers for disturbance attenuation, which successfully damped the disturbance.

Amirhossein, later used this model in [16] to create a MPC controller with feed-forward for disturbance attenuation.

In [2], Edvin Hatlevik, applied linear feed-forward model predictive controller on the model of [17]. This controller was also designed for heave disturbance attenuation. The manipulated variable was the choke valve.

Now a days, researchers approaching advanced nonlinear control techniques to tackles heave motion nonlinearity. One of them is an adaptive backstepping control, which has significant positive impact on performance of the system. Apart from recursive step by step stabilizing approach, which leads to commendable results, its ability to adapt unknown parameters of the system makes it more prominent in control family.

1.3 Problem Statement

1. The controllers implemented on model, given in [17], are internal model controller, and output regulation controller. The output responses of these controllers are not acceptable at all, in transient mode. Even in steady state, down-hole pressure deviates approximately ± 1 *bar* from its desired level.

2. As we are unable to model any physical system as an accurate as ideal; so tackling effect of model uncertainty and variation in parameters is still open research problem in manage pressure drilling system.

3. Uncertainties in hydraulic parameters such as density, rhe-ology of the drilling mud, temperature distribution in the well,frictional pressure

loss for the pipe flow and the annular flow in the well, effective bulk modulus, and well geometry makes drilling even more challenging [18].

1.4 Research Focus

- In the beginning, focus will be on designing nonlinear backstepping controller for MPD system, using Ingar's model, to cancel effect of heave motion effectively.
- Secondly, an adaptive backstepping nonlinear controller will be designed to encounter model uncertainties, to track bottom hole pressure at reference level irrespective of variation in system parameters.
- At the end, to test the authenticity of above mentioned controllers, numerical simulations using MATLAB/Simulink will be used.

1.5 Thesis Outline

The outline of this thesis is as follows. Chapter 2 is devoted to literature review which includes detailed description of drilling process, mathematical modeling and previous implemented controllers on MPD system. Chapter 3 discusses backstepping control design and its stability analysis along with associated simulation results. In chapter 4, adaptive backstepping control has been designed and its associated simulations results are presented. Lastly,chapter 5 concludes the thesis.

Chapter 2

Literature Review

2.1 Drilling System and Process

In Figure 2.1, managed pressure drilling setup on floating rigg is shown and key parts of drilling system are mentioned.

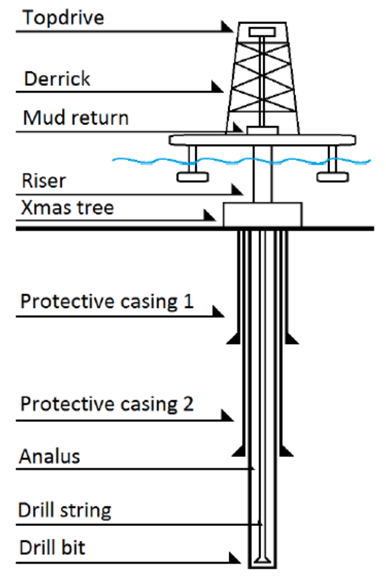

Figure 2.1: Drilling operation [2].

Drill string is assembled with drill tower, also known as derrick; and it is connected with top drive, at the top of derrick. An engine is connected with top drive thats rotates drill string, and it is where, the mud is pumped into the drill string. Drill string and top drive components moved vertically on the derrick, when string goes deeper into the well. In this way, drill string's movement in derrick act as natural heave compensation mechanism of drilling rig. Each drill string is $9m$ long; it is assembled with drill stand, having length of $27m$. When drill string goes into the ground, while drilling operation, a new drilling stand need to connect with last drilled stand. Normally, It takes approximately two hours to drill a drill stand into the ground which means a new stand needs to be added every two hours at normal drill speed. When new pipes required to connect to drill string, the string have to clamped to drill floor. Now, sea waves causes drill bit to act like a piston, in the bottom of the well, due to heave motion.

Mud is pumped into drill string from the mud pit via top drive; it flows out from the drill bit. The mud then carries the drill cuttings up the annulus, as shown in Figure 2.2. From the top of the annulus the return mud flow q_c is controlled by the choke valve. After purification of mud from drill cuttings, in the shale shakers; it is then transported back to the mud pit. The mud plays many important roles in the drilling process, and in the list below are some of its major responsibilities:

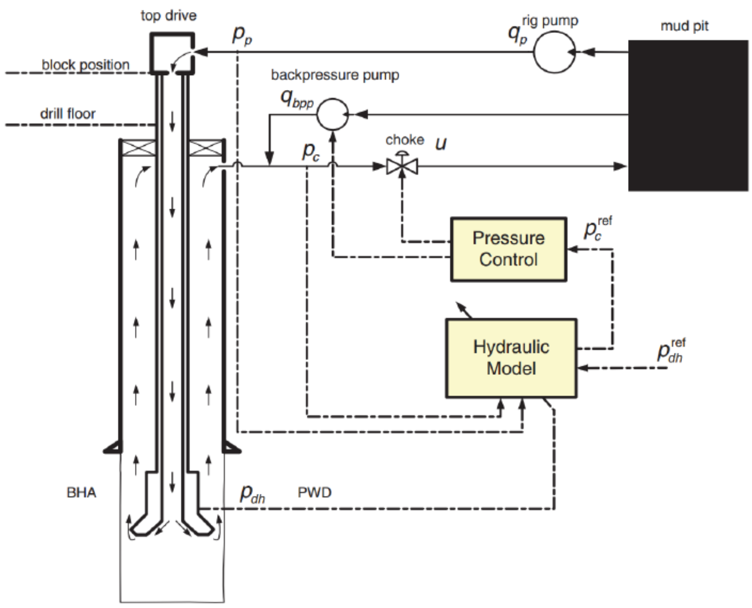

Figure 2.2: Schematic of an automated MPD system [2].

1. When drill cuttings needs to be transported from the drill hole up to the drilling floor. It require's the mud to have rather high viscosity

than drill cuttings in order to be able to bring the cuttings up to the drilling floor. This is described in more detail in [19].

2. During drilling the drill bit may overheat and the mud acts as a coolant for the drill bit.

3. The return flow rate is used in managed pressure drilling to control the bottom-hole pressure.

2.1.1 Pore and fracture pressure

All formation penetrated by the drill bit is to some extent are porous and may contain oil, gas or salt water. Availability of these fluid in the pore space builds up the pore pressure, p_{pore}. It is important to keep the drill pressure p_{bit} higher than the pore pressure. If this criteria is not upheld one of the following situations may occur.

1. If the pressure and the viscosity is to low, gas might leak into the mud creating kicks. Its called kicks because the gas expands as it rises to the surface and creates dangerous increase in pressure and can cause a blow-out.

2. Drilling into neighbouring producing wells.

3. Getting influx to the mud in form of oil or water. This is only wanted during production and may cost both production value and affect the mud's viscosity.

If on the other hand the drill pressure gets higher than a formation's fracture pressure p_{frac} which will cause the mud to leak in to the formation.

1. Mud leaks into the pore space, causing mud loss. This is both costly and in violation of environmental laws.

2. Mud might form a wall over the pores in the drill hole. This problem can be solved by redrilling the area, or it will slow down production.

In short the drill pressure must be held within the pressure range.

$$P_{pore} < P_{bit} < P_{frac} \tag{2.1}$$

Beyond these boundaries are some worst case boundaries.

$$p_{collapse} < P_{pore} < P_{bit} < P_{frac} < p_{overburden} \tag{2.2}$$

The $p_{collapse}$, is the pressure limit where pressure becomes so low that the well will collapse around the drill string. Consequently the drill string may be stuck in the drill hole. $P_{overburden}$ is the combined weight of formation materials and fluids in the geological formations above any particular depth of interest in the earth, [20]. Lastly, it is worth mentioning that the inequality above is not completely written in stone, the $p_{collapse}$ might be larger then the pore pressure in some rare occasions.

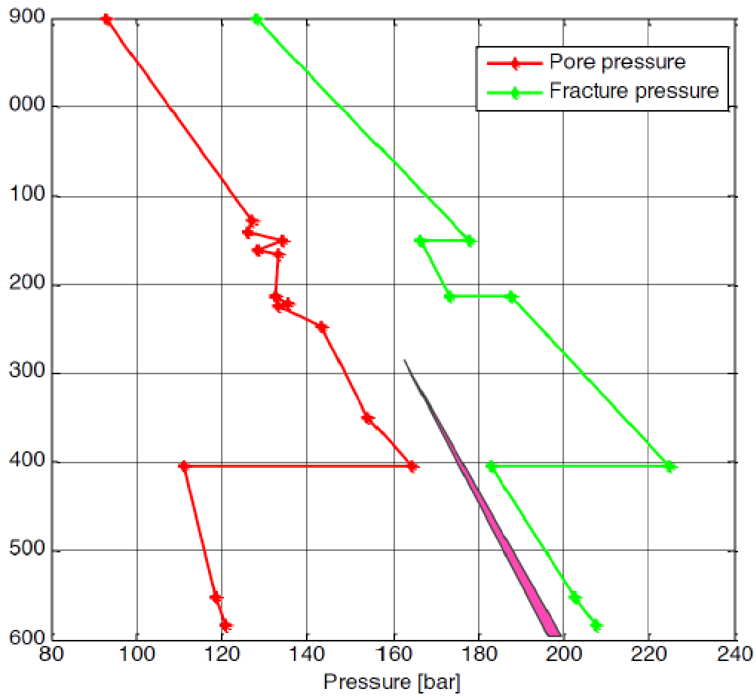

Figure 2.3: Pore and fracture pressures at given depths.(Kaasa, 2012).

The pore and fracture pressure is calculated by geologist prior to the drilling, and can be verified during drilling operations. In figure 2.3, one can see a representation of the possible pressure limits imposed by the pore and fracture pressure, and how the pressure limits is changing with the depth of the well. One of the control objectives are to contain the down hole pressure between the pressure limits calculated by the geologists.

2.1.2 Managed pressure drilling

"Managed Pressure Drilling is an adaptive drilling process used to precisely control the annular pressure profile throughout the wellborn. The objectives are to ascertain the down hole pressure environment limits and to manage the annular hydraulic pressure profile accordingly. The intention of MPD is to avoid continuous influx of formation fluids to the surface. Any influx incidental to the operation will be safely contained using an appropriate process." [19].

2.2 Initial Research on MPD

Initially, A simple mathematical model that represents the major phenomena of drilling system was presented by Kassa in [21]. And later many authors used it for state estimation and control of annular pressure in the well. It can be seen in [12], [13], [22], [14], [23].

In [12], J.Zhou, presented nonlinear adaptive observer and controller to estimate states and to control pressure dynamics. This controller achieved asymptotic stability using feedback control for choke opening and the main pump.

To tackle the problem of well kicks and fluid loss, two years later, J.Zhou, again published an article [13] in which adaptive observer was proposed for kick and loss detection. A switched control system, to control choke valve and back pressure pump, was developed for pressure control and kick attenuation. It successfully ensured the asymptotic convergence for controller. To improve kick management observer was developed to estimate the reservoir pore pressure. The effectiveness of observer and controller was tested by high fidelity drilling simulator.

In [22], Pavlov presented two controller for handling heave motion in MPD operations. The first design was based on feedback linearization, to compensate drill string movement effect on the annular pressure. The second controller, based on feedback linearization and a nonlinear observer, to regulate bottom hole pressure by varying the opening of choke valve. This controller allowed to avoid the risk of pressure wind up due to inherent system delays in long wells and, at the same time, to reduce wear and tear of the choke actuator. The presented experimental results demonstrate good performance of the heave decoupling algorithm. For the heave compensation controller, performance was good for relatively slowly varying drill string velocity. For fast varying drill string movements corresponding to heave motion due to waves, the compensation was not successful.

2.3 Ingar's Mathematical Model for MPD

2.3.1 Hydraulic transmission line modeling

In [17], Ingar had proposed a hydraulic model with finite control volumes to represent the main dynamics of the Ullrig test drilling facility. The model is made for controlling the bottom hole pressure p_{bit} when a new drill stand is being mounted. This results in a model that does not have the mud pump flow because the mud flow through the top drive. Consequently, the only volumetric flow to create a down hole pressure is feedback flow q_{bpp} generated by the back pressure pump.

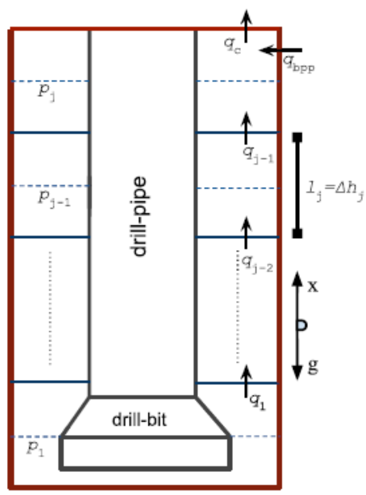

Figure 2.4: Control volumes of the annulus hydraulic model [2].

This resulting hydraulic model is split into two control volumes where each control volume has a differential equation denoting the pressure in this volume and a differential denoting the volumetric flow rate from this volume to the volume above. Each of these control volumes has a volumetric flow rate into control volume and out of the control volume. Where the flow from the up most control volume is determined by the flow through the choke valve q_c, and the flow into the lower control volume is created by the drill bit motion $A_d V_d$.

$$\dot{p_1} = \frac{\beta_1}{A_1 l_1}(-q_1 - v_d A_d)$$
$$\dot{p_i} = \frac{\beta_i}{A_i l_i}(q_{i-1} - q_i) \qquad i = 2, ..., N-1 \tag{2.3}$$
$$\dot{p_N} = \frac{\beta_N}{A_N l_N}(q_{N-1} - q_c + q_b pp)$$

$$\dot{q_i} = \frac{A_i}{l_i \rho_i}(p_i - p_{i+1}) - \frac{F_i(q_i) A_i}{l_i \rho_i} - A_i g \frac{\Delta h_i}{l_i} \tag{2.4}$$
$$i = 1, 2, ..., N-1.$$

Where,

The numbers 1.., N refer to control volume number of annulus where 1 represents the lower most control volume number at bottom of the well; so p_1 represents bottom-hole pressure. The control volume number N represents the upper most volume number; therefore, p_N denotes pressure at the top of the annulus, which means choke pressure. Similarly, q_i represents the mud flow in i^{th} control volume and in uppermost control volume the return mud flow is represented by q_c as in uppermost control volume return mud flow is flowing through choke valve.

According to system's manipulated variables one can control bottom-hole pressure using back-pressure pump and the choke valve. In case of back-pressure pump control, it will be required for back-pressure pump to change speed enough that could change-hole pressure faster than sea waves. But it is not possible for pump to change its speed so fast so the choke valve is mainly used for pressure control. And the parameters are defined as.

- β_i: The bulk modulus of the mud in control volume i.
- A_i: Is the cross section area in control volume i .
- l_i: Length of each control volume i .
- Δh_i: Height of each control volume i .
- ρ_i: Mud density in control volume i .
- $F_i(q_i)$: Friction force in the control volume i.
- g: Acceleration of gravity.
- v_d: Heave velocity due to ocean waves.

2.3.2 Choke valve

To have a control system one must have a manipulated variable. In a MPD systems its common to control the annulus return flow in order to control the bottom-hole pressure. Back pressure pump flow q_{bpp} and mud return flow q_c can be controlled, at exit point, to control return flow. Pump frequency and q_{bpp} are linearly related so one cannot change backpressure pump fast enough to accommodate heave-induced pressure oscillations. As a result, one can control return flow by controlling choke flow rate q_c. It is modeled by the orifice equation which is given as [17].

$$q_c = K_c \sqrt{p_c - p_0} G(u) \tag{2.5}$$

Where,

- K_c: Choke constant represents choke area mud density.
- p_0: Atmospheric pressure.
- $G(u)$: Strictly increasing and invertible function relating the control signal to the actual choke opening.

Choke characteristic are nonlinear in nature. This one cant be linearised directly but by using feedback linearisation; this non-linearity can also be removed in order to create a linear system.

$$\begin{aligned} u_a &= q_{bpp} - q_c \\ u_a &= q_{bpp} - K_c \sqrt{p_c - p_0} G(u) \\ G(u) &= \frac{q_b pp - u_a}{K_c \sqrt{p_c - p_0}} \end{aligned} \tag{2.6}$$

As back-pressure pump flow has a severe rate limitation, so control strategy is to keep q_{bpp} at a constant level and using the choke valve we will cancel out the effect of heave motion (pressure oscillation). The constant q_{bpp} is thus chosen in such a way the bottom-hole pressure is equal to the desired pressure when the wave disturbance v_d is *zero m* and the choke opening percentage is at 50 percent [17].

2.3.3 Friction model

Based on experimental research from the Ullrig test data, the friction force in annulus can be considered as a linear function [24].

$$
\begin{aligned}
F_i(q_i) &= \frac{k_{fric,i} q_i}{A_i} \\
k_{fric,i} &= \frac{64 l_i u_i (\alpha_i + \beta_i)}{r_h, i^2}
\end{aligned}
\tag{2.7}
$$

Where,

The new parameters are defined as:

- u_i is the viscosity in the specific control volume.
- α_i and β_i are constants.
- r_h is the hydraulic radius.

2.3.4 Heave motion model

To model the relative drill string movement, one must have the information of waves behaviour in North Atlantic, which causes to move drill string dangerously. According to [24], [17] and [16], heave motion can be modeled by equation 2.8, as $\frac{\pi}{6}$ is close to dominant frequency of sea waves in North ocean.

$$v_d = 1.0 cos(\frac{\pi}{6} t) \tag{2.8}$$

With reference to JONSWAP spectrum, the amplitude of sea waves normally remained at 1 m. With this model many researchers have worked on MPD [24], [16].

To analyse the effect of sea waves on managed pressure drilling process, in the presence of other waves already disturbing drilling process, a new heave motion model is proposed. In this model, the amplitude of sinusoidal wave form is varied sinusoidally. The proposed model is given below.

$$v_d = A cos(\frac{\pi}{x} t) cos(\frac{\pi}{6} t) \tag{2.9}$$

Where, A is representing amplitude of sinusoidally varying sinusoidal; and x represents how many times we want to sinusoidally amplitude of heave motion.

2.3.5 State space model

In this section, statespace model of discussed system is presented. And parameters are redefined in more simpler fashion according to following rule:

$$a_j = \frac{\beta_j}{A_j l_j}, \quad b_j = \frac{A_j}{\rho_j l_j}, \quad c_j = \frac{k_{frick}}{\rho_j l_j}, \quad e_j = \frac{A_j g \Delta h_j}{l_j} \tag{2.10}$$

Subtituting 2.10 in 2.3 and 2.4, the resulting model which get is given as:

$$\begin{aligned} \dot{p_1} &= -a_1 q_1 - a_1 A_d v_d \\ \dot{p_i} &= a_i q_{i-1} - a_i q_i \qquad i = 2, ..., N-1 \\ \dot{p_N} &= a_N q_{N-1} + a_N u_a \end{aligned} \tag{2.11}$$

$$\begin{aligned} &\dot{q_i} = b_i p_i - b_i p_{i+1} - c_i q_i - e_i \\ &i = 1, 2, ..., N-1. \end{aligned} \tag{2.12}$$

According to Ingar, he had derived models for two and five control volumes. In this thesis, model having two control volumes, where ($N = 2$) is used then the resulting model can be written as:

$$\begin{aligned} \dot{p_1} &= -a_1 q_1 - a_1 A_d v_d \\ \dot{p_2} &= a_2 q_1 - a_2 u_a \\ \dot{q_1} &= b_1 p_1 - b_1 p_2 - c_1 q_1 - e_1 \end{aligned} \tag{2.13}$$

To make this dynamical model more simple, state variable transformation is used in which p_1, q_1 and p_2 are replaced with x_1, x_2 and x_3 respectively; then the resulting system will be in given below form:

$$\begin{aligned} \dot{x_1} &= -a_1 x_2 - a_1 A_d v_d \\ \dot{x_2} &= b_1 x_1 - b_1 x_3 - c_1 x_2 - e_1 \\ \dot{x_3} &= a_2 x_2 - a_2 u_a \end{aligned} \tag{2.14}$$

In this final transformed model x_1 represents bottom-hole pressure, x_2 represents mud flow in bottom of well, near drill-bit and x_3 denotes choke pressure, near the top of annulus. And u_a is representing addition of choke flow and back-pressure pump flow; and it is the variable which is required to control, to regulate x_1 at desired level.

The well is assumed to be 1990.99m long and the system parameters re identified from IRIS Drill simulator [16]. The system parameters are defined in Table 2.1; authors have used these parameters in [17], [2].

Parameters	Value		Parameters	Value	
a_i	2.254 x10^8	$[P_a/m^3]$	A_d	0.291	$[m^2]$
b_i	4.28 x10^{-8}	$[m^4/K_g]$	q_{bpp}	369.2464	$[m^3/s]$
c_i	14.5	$[1/sm^2]$	p_0	101325	[Pa]
e_i	0.2638	$[m^3/s^2]$	K_c	2.32	

Table 2.1: System Parameters Value.

2.4 Error Dynamical Model

Ingar's mathematical model of MPD system is being used in this thesis, as discussed in previous chapter is given below [17]:

$$\begin{aligned} \dot{x_1} &= -a_1 x_2 - a_1 A_d v_d \\ \dot{x_2} &= b_1 x_1 - b_1 x_3 - c_1 x_2 - e_1 \\ \dot{x_3} &= a_2 x_2 - a_2 u_a \end{aligned} \tag{2.15}$$

Backstepping and Adaptive backstepping control algorithms can be applied on only strict feedback systems and the above system is in this form. So, using these control techniques, control input u_a will be designed to regulate bottom hole pressure along with damping the effect of heave motion. The strategy is to modify system's dynamics into error dynamics of that system. Then throughout the procedure, objective will be to design such control u_a that ensure system's error dynamics are converging. Rules for state variables transformation are described as:

$$\begin{aligned} z_1 &= x_1 - x_d \\ z_2 &= x_2 - \alpha_1 \\ z_3 &= x_3 - \alpha_2 \end{aligned} \tag{2.16}$$

Where x_d is desired set point and α_1 and α_2 are virtual control inputs. By calculating derivatives of 2.16, we get

$$\begin{aligned} \dot{z_1} &= \dot{x_1} - \dot{x_d} \\ \dot{z_2} &= \dot{x_2} - \dot{\alpha_1} \\ \dot{z_3} &= \dot{x_3} - \dot{\alpha_2} \end{aligned} \tag{2.17}$$

Now by substituting 2.15 into 2.17; system's error dynamics can be calculated as:

$$\begin{aligned} \dot{z_1} &= -a_1(z_2 + \alpha_1) - a_1 A_d v_d - \dot{x_d} \\ \dot{z_2} &= +b_1(z_1 + x_d) - b_1(z_3 + \alpha_2) - c_1(z_2 + \alpha_1) - e_1 - \dot{\alpha_1} \\ \dot{z_3} &= +a_2(z_2 + \alpha_1) - a_2 u_a - \dot{\alpha_2} \end{aligned} \tag{2.18}$$

Where,

The errors dynamics of the system are represented by z_1, z_2 and z_3. Control input u_a should be able enough to make sure that these error trajectories are converging. One can design control input u_a, using any desired control algorithm, according to system dynamics, to achieve required objectives; however, in this thesis, u_a is designed using backstepping and adaptive backstepping control algorithms.

2.5 Latest Research on MPD

Ingar Skyberg Landet considered the problem of compensation of heave-induced pressure oscillations in MPD operations, in 2013 [17]. Firstly, the new dynamical model was presented which includes detailed friction and heave-motion information. New mathematical model was tested against data from full-scale tests.

Along with presenting new mathematical model, Ingar also proposed linear model controller and output regulation controller, in the same paper. The later controller remained more successful in term of pressure fluctuation suppression in comparison with linear internal model controller.

Only two months later, Amirhossein Nikoofard [16], used the same model designed by [17], to successfully control the downhole pressure using constrained model predictive control. It was concluded that a constrained MPC showed improved attenuation of the heave disturbance.

In end of 2016, Hessam, proposed nonlinear controller based on output regulation theory. To deal with choke nonlinearity it uses nonlinear inversion element which is connected with adaptive compensator and output feedback controller [25]. Hessam, published another article based on L_1 adaptive control theory for managed pressure drillng [18], a couple of months ago.

Chapter 3

Backstepping Control Design and Simulation Results

3.1 Control Design Procedure and Stability Analysis

Backstepping control is advanced nonlinear control technique; it has ability to tackle matched disturbance effectively, in dynamical systems. Backstepping control design procedure remain simple even for higher order models as it is a step by step implementation procedure. While designing this control, lyapnov stability ensures system dynamics convergence, at each step. A complete control design procedure include following three steps:

- **Step: 1**

  In the beginning, the lyapnov function V_1, for z_1 trajectory, is defined; then, after calculating it's derivative, the value of $\dot{z}_1$ is substituted in it, using 2.18. The resulting equations are given below:

$$\begin{aligned} V_1 &= \frac{1}{2} z_1^2 \\ \dot{V}_1 &= z_1 \dot{z}_1 \\ \dot{V}_1 &= z_1(-a_1(z_2 + \alpha_1) - a_1 A_d v_d - \dot{x}_d) \\ \dot{V}_1 &= -a_1 z_1 z_2 - a_1 \alpha_1 z_1 - a_1 A_d v_d z_1 - z_1 \dot{x}_d) \end{aligned} \tag{3.1}$$

  To ensure that the rate of change of above calculated energy function, for z_1 trajectory, is converging towards zero; then $\dot{V}_1$ has to be decreasing function, for any value of z_1. So, to meet said objective, the virtual control α_1 is designed by replacing $\dot{V}_1$ with $-c_{11}z_1^2$, in 3.1. Where, c_{11} is virtual control gain, the value of this gain determine how fast trajectory of z_1 is converging.

$$
\begin{aligned}
-c_{11}z_1^2 &= -a_1\alpha_1 z_1 - a_1 A_d v_d z_1 - z_1\dot{x_d}) \\
-c_{11}z_1 &= -a_1\alpha_1 - a_1 A_d v_d - \dot{x_d}) \\
\alpha_1 &= \frac{c_{11}}{a_1}z_1 - AdVd - \frac{1}{a_1}\dot{x_d}
\end{aligned}
\tag{3.2}
$$

After substituting virtual control α_1 into 3.1; we have given below resulting equation.

$$
\dot{V}_1 = -c_{11}z_1^2 - a_1 z_1 z_2 \tag{3.3}
$$

The equation 3.3 represents that the z_1 state is converging towards *zero*, irrespective of its initial condition; however, virtual control α_1 is not ensuring z_2 trajectory to converge. To force z_2 state to converge, another virtual control α_2 will be designed in next step.

- **Step: 2**

In this step, the lyapnov function V_2 is defined, which is combination of V_1 and energy function of z_2 state; then, after calculating it's derivative, the value of $\dot{z}_2$ and $\dot{V}_1$ are substituted in it, using 2.18 and 3.3, respectively. The resulting equations are given below:

$$
\begin{aligned}
V_2 &= +V_1 + \frac{1}{2}z_2^2 \\
\dot{V}_2 &= +\dot{V}_1 + z_2\dot{z}_2 \\
\dot{V}_2 &= -c_{11}z_1^2 - a_1 z_1 z_2 + z_2(b_1(z_1 + x_d) \\
&\quad - b_1(z_3 + \alpha_2) - c_1(z_2 + \alpha_1) - e_1 - \dot{\alpha_1}) \\
\dot{V}_2 &= -c_{11}z_1^2 - a_1 z_1 z_2 + b_1 z_1 z_2 + b_1 x_d z_2 - b_1 z_2 z_3 \\
&\quad - b_1 z_2 \alpha_2 - c_1 z_2^2 - c_1 z_2 \alpha_1 - e_1 z_2 - z_2\dot{\alpha_1}
\end{aligned}
\tag{3.4}
$$

To ensure convergence behaviour of z_1 z_2 trajectories, rate of change of above calculated energy function $\dot{V}_2$ has to be decreasing for all values of z_1 and z_2 states. So, to meet said objective, the virtual control input α_2 is designed by replacing $\dot{V}_2$ with $-c_{12}z_2^2$, in 3.4. Where, c_{12} is virtual control gain; the value of this gain determine how fast trajectory of z_2

is converging.

$$
\begin{aligned}
-c_{12}z_2^2 &= -a_1z_1z_2 + b_1z_1z_2 + b_1x_dz_2 - b_1z_2\alpha_2 - c_1z_2^2 - c_1z_2\alpha_1 \\
&\quad - e_1z_2 - z_2\dot{\alpha_1} \\
-c_{12}z_2 &= -a_1z_1 + b_1z_1 + b_1x_d - b_1\alpha_2 - c_1z_2 - c_1\alpha_1 - e_1 - \dot{\alpha_1} \\
\alpha_2 &= \frac{c_{12}-c_1}{b_1}z_2 + \frac{b_1-a_1}{b_1}z_1 - \frac{c_1}{b_1}\alpha_1 - \frac{e_1}{b_1} + x_d - \frac{\dot{\alpha_1}}{b_1}
\end{aligned} \tag{3.5}
$$

Now by substituting virtual control α_2 into 3.4, the resulting equation equation is given below.

$$\dot{V_2} = -c_{11}z_1^2 - c_{12}z_2^2 - b_1z_2z_3 \tag{3.6}$$

The equation 3.6 represents that the z_1 and z_2 states are converging towards zero, irrespective of their initial conditions; however, virtual control α_2 is not forcing the trajectory of z_3 to move towards *zero*. To force z_3 state to converge, actual control u_a will be designed in last step.

- **Step: 3**

In last step, the lyapnov function V_3 is defined, which is combination of V_2 and energy function of z_3 state; then, after calculating it's derivative, the values of $\dot{z_3}$ and $\dot{V_2}$ are substituted in it, using 2.18 and 3.6, respectively. The resulting equations are given below:

$$
\begin{aligned}
V_3 &= V_2 + \frac{1}{2}z_3^2 \\
\dot{V_3} &= \dot{V_2} + z_3\dot{z_3} \\
\dot{V_3} &= -c_{11}z_1^2 - c_{12}z_2^2 - b_1z_2z_3 + z_3\dot{z_3} \\
\dot{V_3} &= -c_{11}z_1^2 - c_{12}z_2^2 - b_1z_2z_3 + z_3(a_2(z_2+\alpha_1) - a_2u_a - \dot{\alpha_2}) \\
\dot{V_3} &= -c_{11}z_1^2 - c_{12}z_2^2 - b_1z_2z_3 + a_2z_2z_3 + a_2\alpha_1z_3 - a_2u_az_3 - \dot{\alpha_2}z_3
\end{aligned} \tag{3.7}
$$

To ensure convergence behaviour of all system trajectories, rate of change of above calculated energy function $\dot{V_3}$ has to be decreasing for all values of z_1, z_2 and z_3 states. So, to meet said objective, the actual control input u_a is designed by replacing $\dot{V_3}$ with $-c_{13}z_3^3$, in 3.7. Where, c_{13} is actual control gain, the value of this gain determine how fast trajectory of z_3 is converging. This remaining procedure is presented below:

$$\begin{aligned}
-c_{13}z_3^2 &= -b_1z_2z_3 + a_2z_2z_3 + a_2\alpha_1z_3 - a_2u_az_3 - \dot{\alpha}_2z_3 \\
-c_{13}z_3 &= -b_1z_2 + a_2z_2 + a_2\alpha_1 - a_2u_a - \dot{\alpha}_2 \\
u_a &= \frac{c_{13}}{a_2}z_3 - \frac{b_1}{a_2}z_2 + z_2 + \alpha_1 - \frac{1}{a_2}\dot{\alpha}_2
\end{aligned} \tag{3.8}$$

Now by substituting actual control u_a into 3.7; and the resulting equation is given below.

$$\dot{V}_3 = -c_{11}z_1^2 - c_{12}z_2^2 - c_{13}z_3^2 \tag{3.9}$$

The equation 3.9 represents that all z_1, z_2 and z_3 states are converging towards *zero*, irrespective of their initial conditions.

3.2 Simulation Results

To demonstrate the effectiveness of the proposed controller, simulation is performed using system error dynamical model and disturbance model, discussed in previous chapter, and assuming perfect conditions. That is, we can measure all states and heave motion, while drilling operation. Design requirements were to track bottom hole pressure at 218 *bar*.

3.2.1 Sinusoidal heave motion with one meter amplitude

From figures 3.1-3.3, three wave forms are shown, which represents heave motion, bottom-hole pressure and choke opening percentage, respectively. As it is clear from results, backstepping controller achieved asymptotic rejection of heave disturbance. In the the presence of 1 *m* sinusoidal heave motion, backstepping controller has restricted bottom-hole pressure within window of 0.15 *bar*, in steady state. With small spike in transient, control choke remains almost 50 percent open, throughout the simulation.

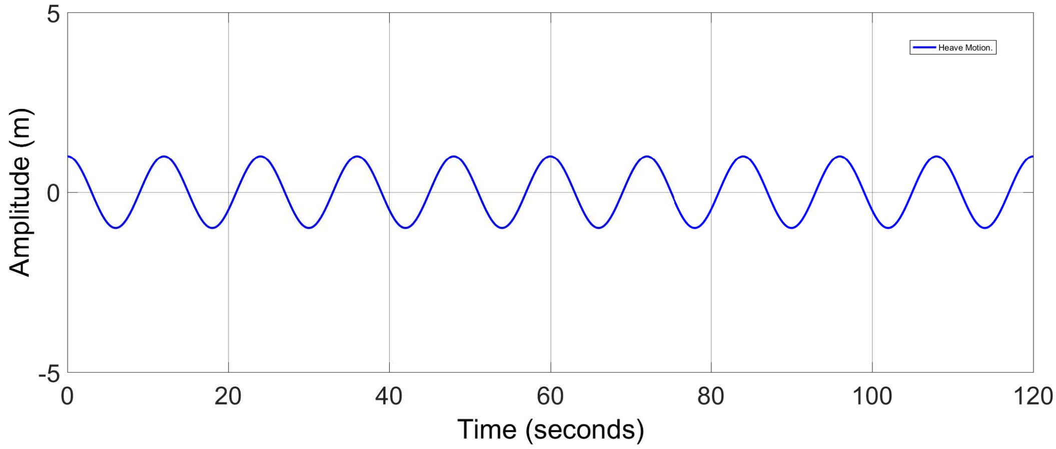

Figure 3.1: Heave Disturbance.

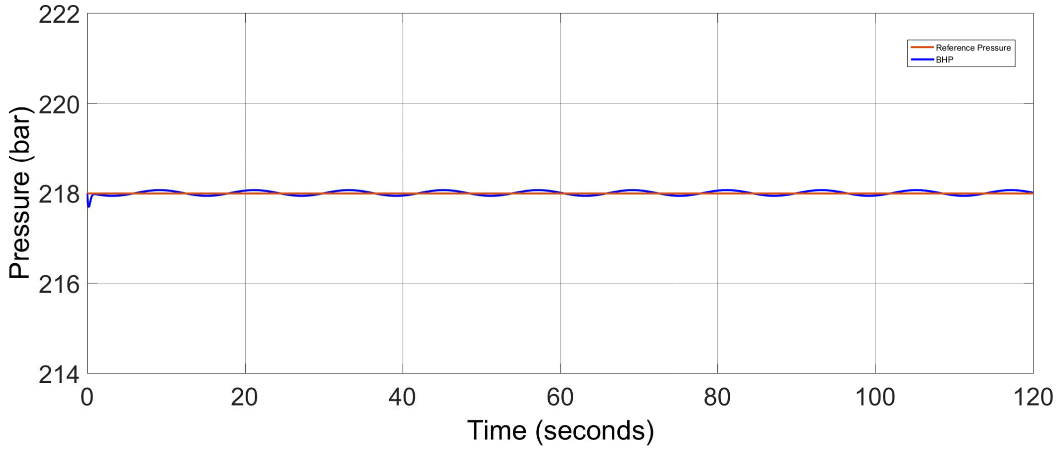

Figure 3.2: Bottom-hole Pressure.

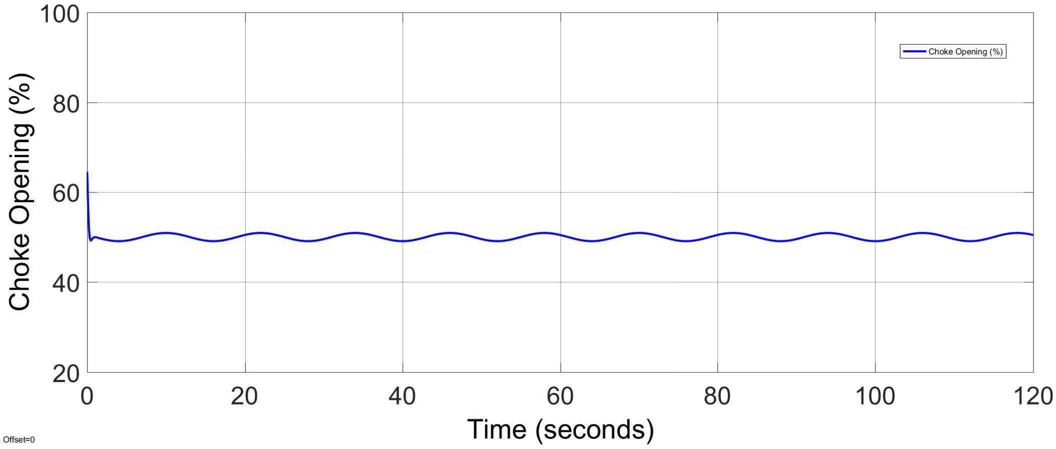

Figure 3.3: Choke Opening Percentage.

3.2.2 Sinusoidal heave motion with three meter amplitude

Normally, the amplitude of heave motion remain around 3 m; so controller is tested with heave motion having 3 m amplitude. With reference to figures 3.4-3.6, backstepping controller remain best in term of suppression of oscillations. In comparison with previous case, bottom-hole pressure has 0.5 peak-to-peak oscillations but these are more than acceptable. As according to [16], oscillations within ± 2.5 *bar* are acceptable, in even complex in deep sea managed pressure drilling.

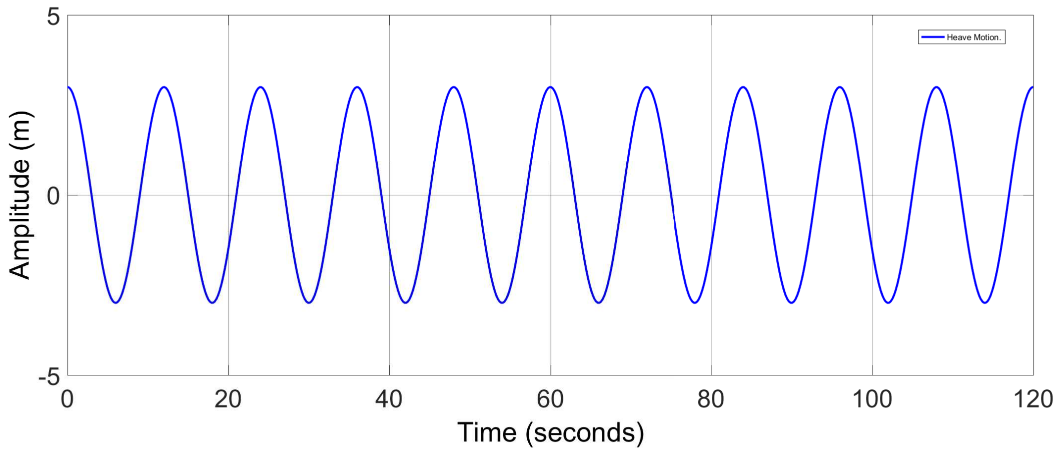

Figure 3.4: Heave Disturbance.

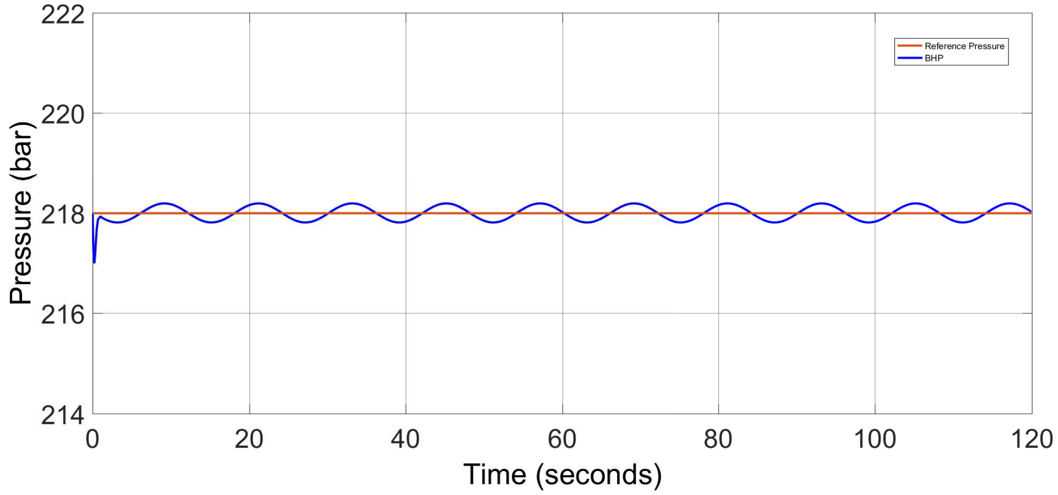

Figure 3.5: Bottom-hole Pressure.

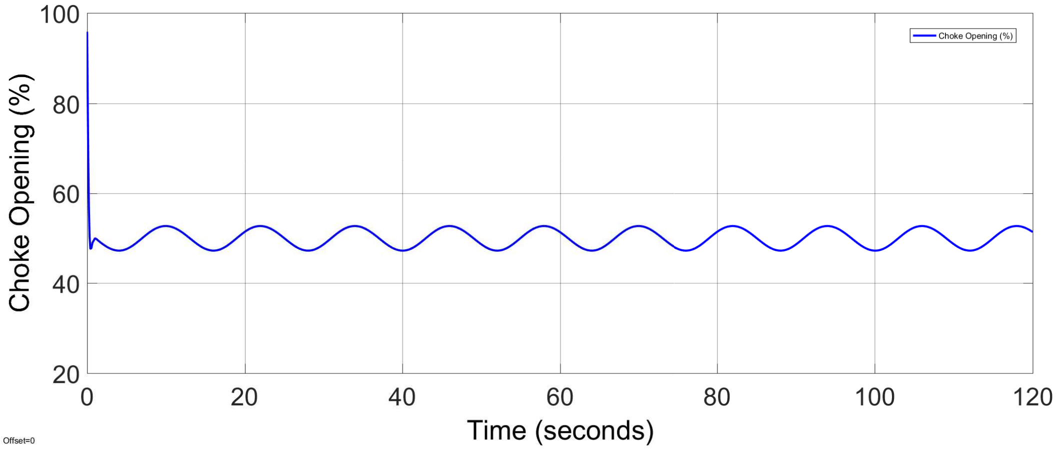

Figure 3.6: Choke Opening Percentage.

3.2.3 Sinusoidal heave motion with one meter sinusoidally varying amplitude

As amplitude of heave motion can change due to severe weather conditions, during operation. So to check controller performance in more realistic way, a sinusoidal wave having sinusoidally varying amplitude is being used. From figure 3.7-3.9, three wave forms are shown, which represents heave motion, bottom-hole pressure and choke opening percentage, respectively. In this scenario, the results are almost similar with the result of 4.2.1.

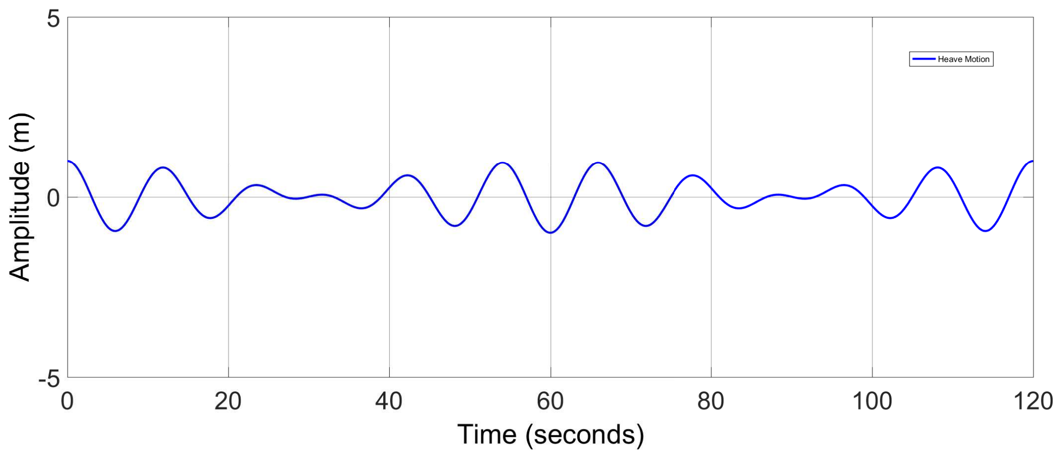

Figure 3.7: Heave Disturbance.

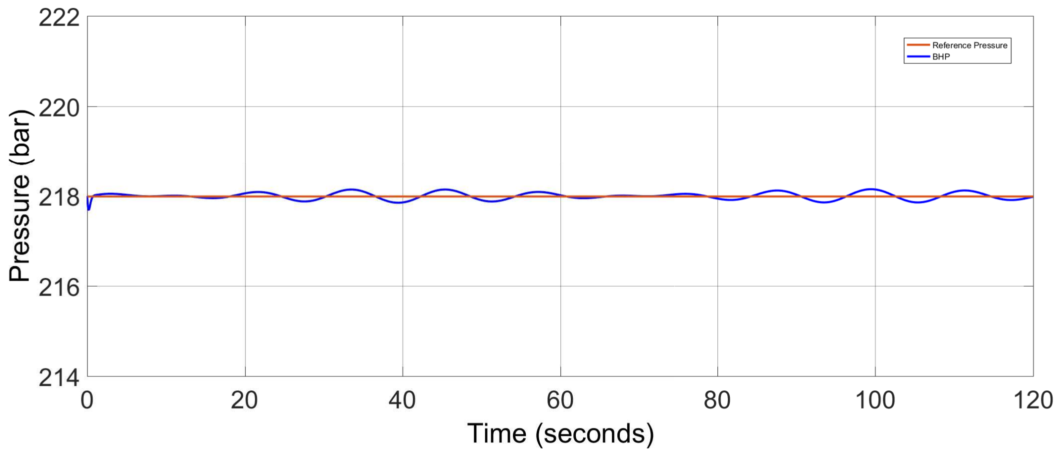

Figure 3.8: Bottom-hole Pressure.

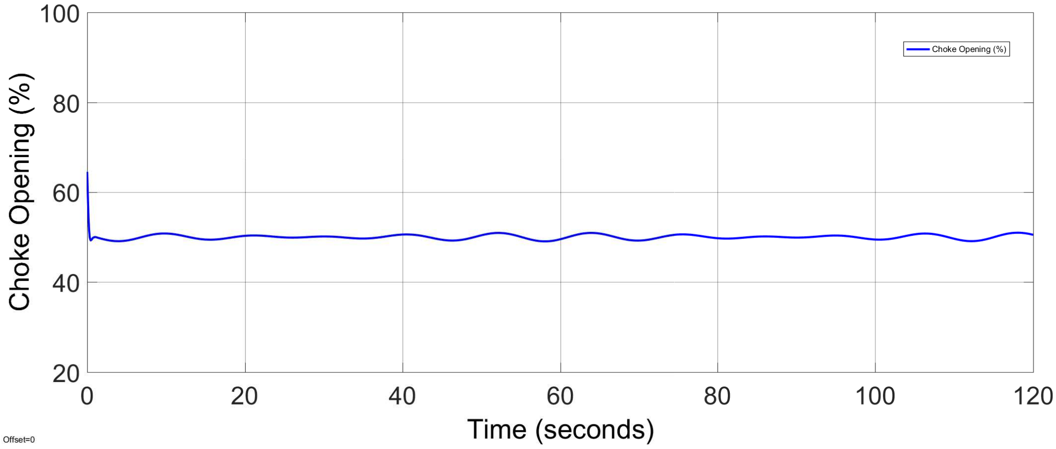

Figure 3.9: Choke Opening Percentage.

3.2.4 Sinusoidal heave motion with three meter sinusoidally varying amplitude

From figure 3.10-3.12, three wave forms are shown, which represents heave motion, bottom-hole pressure and choke opening percentage, respectively. In this scenario the results are same as they were in section 4.2.1. A small difference in shape of bottom hole pressure is observed which is due to the shape of heave motion.

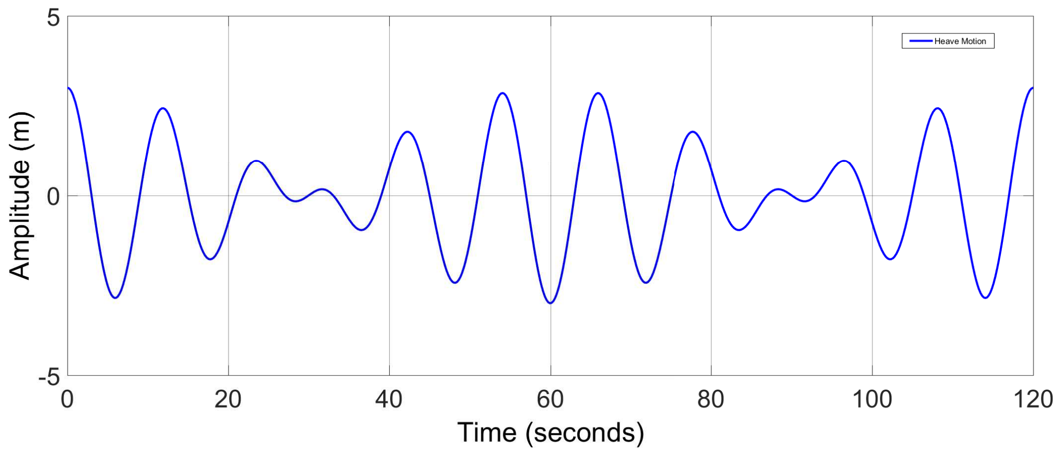

Figure 3.10: Heave Disturbance.

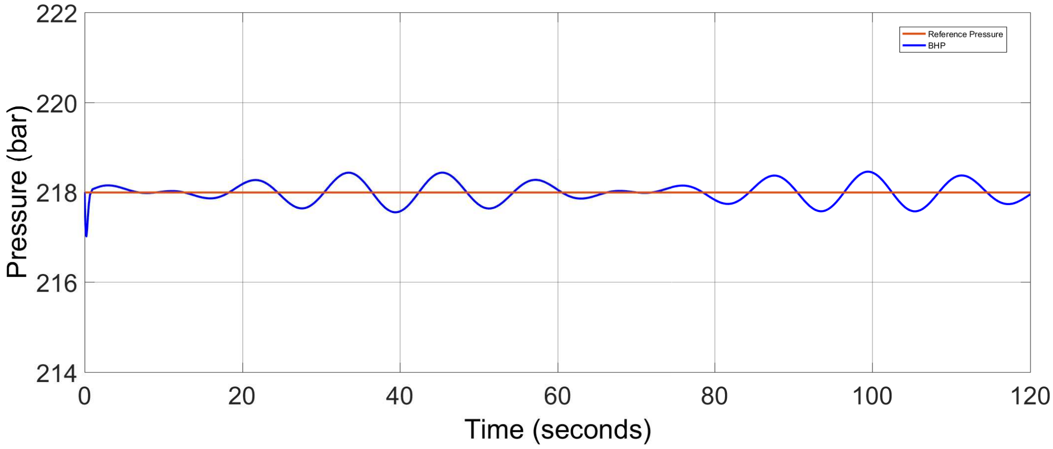

Figure 3.11: Bottom-hole Pressure.

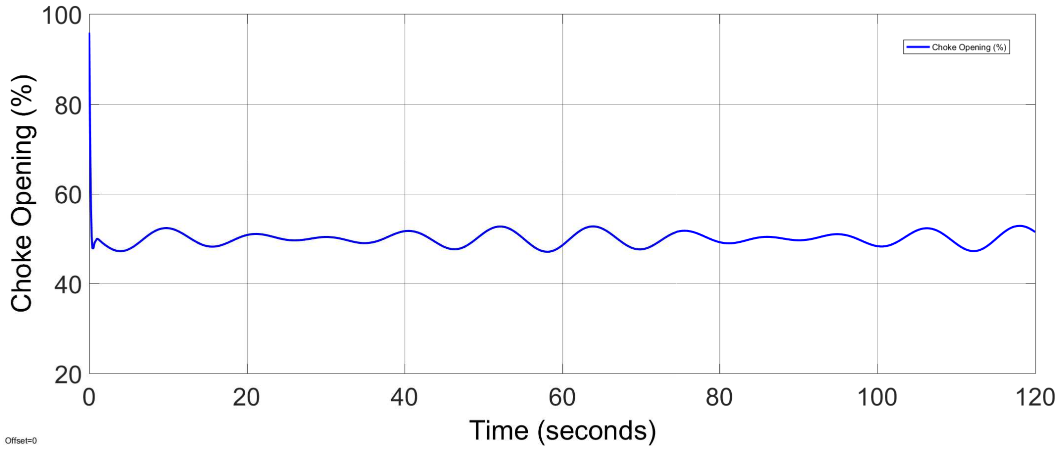

Figure 3.12: Choke Opening Percentage.

Chapter 4

Adaptive Backstepping Control and Simulation Results

4.1 Control Design Procedure and Stability Analysis

In complicated systems, there are often parameters which are not fully known, or which might even occasionally change. To cope with this, an adaptive controller is better choice, as it has significant positive impact on performance of the system. Apart from recursive step by step stabilizing approach of that controller which leads to commendable results, its ability to adapt unknown parameters of system makes it more prominent in controllers family. In this section, an adaptive backstepping controller is proposed in which this controller controls bottom-hole pressure, in presence of time-varying parameter a_1. The strategy is to estimate a_1 parameter first then designing of control algorithm, for system described in 2.18. Control input u_a will be designed by considering estimated parameter $\hat{a_1}$, instead of constant a_1. A complete design procedure including five steps is given below:

- **Step 1: Defining time-varying parameter's error:**

  The actual and estimated value of unknown time-varying parameter of the system is represented by a_1 and $\hat{a}$ simultaneously. And the error between actual and estimated parameter and its derivative is defined below.

$$\begin{aligned} \tilde{a} &= a_1 - \hat{a_1} \\ \dot{\tilde{a_1}} &= -\dot{\hat{a_1}} \end{aligned} \tag{4.1}$$

- **Step 2: Tuning function:**

  Using adaptive backstepping algorithm rate of change of estimated parameter is presented here:

$$\begin{aligned} w_1 &= f_1 = -x_2 - A_d v_d = -(z_2 + \alpha_1) - A_d v_d \\ \tau_1 &= z_1 w_1 = z_1(-(z_2 + \alpha_1) - A_d v_d) \\ \dot{\hat{a}}_1 &= r\tau_1 = r z_1(-z_2 - \alpha_1 - A_d v_d) \end{aligned} \tag{4.2}$$

- **Step: 3**

  In the beginning, the lyapnov function V_1 is defined to represent the trajectories of z_1 and $\tilde{a_1}$; then, after calculating it's derivative, the value of $\dot{z_1}$ and $\dot{\hat{a_1}}$ is substituted in it, using 2.18, 4.1 and 4.2. The resulting equations are given below:

$$\begin{aligned} V_1 &= \frac{1}{2}z_1^2 + \frac{1}{2r}\tilde{a}_1^2 \\ \dot{V_1} &= z_1\dot{z_1} + \frac{1}{r}\tilde{a_1}\dot{\hat{a_1}} \\ \dot{V_1} &= z_1(-a_1(z_2 + \alpha_1) - a_1 A_d v_d - \dot{x_d}) - \frac{1}{r}(a_1 - \hat{a_1})(\dot{\hat{a_1}}) \\ \dot{V_1} &= z_1(-a_1(z_2 + \alpha_1) - a_1 A_d v_d - \dot{x_d}) - (a_1 - \hat{a_1})z_1(-z_2 - \alpha_1 - A_d v_d) \\ \dot{V_1} &= z_1(-a_1(z_2 + \alpha_1) - a_1 A_d v_d - \dot{x_d}) - (a_1 - \hat{a_1})z_1(-z_2 - \alpha_1 - A_d v_d) \\ \dot{V_1} &= -a_1(z_1z_2 + z_1\alpha_1 + z_1 A_d v_d) - z_1\dot{x_d} + a_1(z_1z_2 + z_1\alpha_1 + z_1 A_d v_d) \\ &\quad - \hat{a_1}(z_1z_2 + z_1\alpha_1 + z_1 A_d v_d) \\ \dot{V_1} &= -\hat{a_1}(z_1z_2 + z_1\alpha_1 + z_1 A_d v_d) - z_1\dot{x_d} \\ \dot{V_1} &= -\hat{a_1}z_1z_2 - \hat{a_1}z_1\alpha_1 - \hat{a_1}z_1 A_d v_d - z_1\dot{x_d} \end{aligned} \tag{4.3}$$

  To ensure that the rate of change of above calculated energy function, for z_1 trajectory, is converging towards zero; then $\dot{V_1}$ has to be decreasing function, for any value of z_1. So, to meet said objective, the virtual control input α_1 is designed by replacing $\dot{V_1}$ with $-c_{11}z_1^2$, in 4.3. Where, c_{11} is virtual control gain, the value of this gain determine how fast trajectory of z_1 is converging. The remaining calculations are given below.

$$
\begin{aligned}
-c_{11}z_1^2 &= -\hat{a_1}\alpha_1 z_1 - \hat{a_1}A_d v_d z_1 - z_1\dot{x_d}) \\
-c_{11}z_1 &= -\hat{a_1}\alpha_1 - \hat{a_1}A_d v_d - \dot{x_d}) \\
\alpha_1 &= \frac{c_{11}}{\hat{a_1}}z_1 - A_d v_d - \frac{1}{\hat{a_1}}\dot{x_d}
\end{aligned} \tag{4.4}
$$

Now by substituting virtual control α_1 into 4.3; we get following equation.

$$\dot{V_1} = -c_{11}z_1^2 - \hat{a_1}z_1 z_2 \tag{4.5}$$

The equation 4.5 represents that the z_1 state is converging towards zero; and it is independent from initial conditions. However, virtual control α_1 is not ensuring z_2 trajectory to converge. To force z_2 state to converge, another virtual control α_2 will be designed in next step.

- **Step: 4**

In this step, the lyapnov function V_2 is defined, which is combination of V_1 and energy function of z_2 state; then, after calculating it's derivative, the value of $\dot{z_2}$ and $\dot{V_1}$ are substituted in it, using 2.18 and 4.5, respectively. The resulting equations are given below.

$$
\begin{aligned}
V_2 &= +V_1 + \frac{1}{2}z_2^2 \\
\dot{V_2} &= +\dot{V_1} + z_2\dot{z_2} \\
\dot{V_2} &= -c_{11}z_1^2 - \hat{a_1}z_1 z_2 + z_2(b_1(z_1 + x_d) \\
&\quad - b_1(z_3 + \alpha_2) - c_1(z_2 + \alpha_1) - e_1 - \dot{\alpha_1}) \\
\dot{V_2} &= -c_{11}z_1^2 - \hat{a_1}z_1 z_2 + b_1 z_1 z_2 + b_1 x_d z_2 - b_1 z_2 z_3 \\
&\quad - b_1 z_2 \alpha_2 - c_1 z_2^2 - c_1 z_2 \alpha_1 - e_1 z_2 - z_2\dot{\alpha_1}
\end{aligned} \tag{4.6}
$$

To ensure convergence behaviour of z_1 and z_2 trajectories, rate of change of above calculated energy function $\dot{V_2}$ has to be decreasing, for all values of z_1 and z_2 states. So, to meet said objective, the virtual control input α_2 is designed by replacing $\dot{V_2}$ with $-c_{12}z_2^2$, in 4.6. Where, c_{12} is virtual control gain, the value of this gain determine how fast trajectory of z_2 is converging. The remaining procedure is presented below:

$$
\begin{aligned}
-c_{12}z_2^2 &= -\hat{a}_1 z_1 z_2 + b_1 z_1 z_2 + b_1 x_d z_2 - b_1 z_2 \alpha_2 - c_1 z_2^2 - c_1 z_2 \alpha_1 \\
&\quad - e_1 z_2 - z_2 \dot{\alpha}_1 \\
-c_{12}z_2 &= -\hat{a}_1 z_1 + b_1 z_1 + b_1 x_d - b_1 \alpha_2 - c_1 z_2 - c_1 \alpha_1 - e_1 - \dot{\alpha}_1 \quad (4.7) \\
\alpha_2 &= \frac{c_{12} - c_1}{b_1} z_2 + \frac{b_1 - \hat{a}_1}{b_1} z_1 - \frac{c_1}{b_1}\alpha_1 - \frac{e_1}{b_1} + x_d - \frac{\dot{\alpha}_1}{b_1}
\end{aligned}
$$

Substituting virtual control α_2 into 4.6, we get following equation.

$$\dot{V}_2 = -c_{11}z_1^2 - c_{12}z_2^2 - b_1 z_2 z_3 \tag{4.8}$$

The equation 4.8 represents that the z_1 and z_2 states are converging towards *zero*, irrespective of their initial conditions; however, virtual control α_2 is not forcing the trajectory of z_3 to move towards *zero*. To force z_3 state to converge, actual control u_a will be designed in last step.

- **Step: 5**

In last step, the lyapnov function V_3 is defined, which is combination of V_2 and energy function of z_3 state; then, after calculating it's derivative, the value of $\dot{z_3}$ and $\dot{V_2}$ are substituted in it, using 2.18 and 4.8, respectively. The resulting equations are given below:

$$
\begin{aligned}
V_3 &= V_2 + \frac{1}{2}z_3^2 \\
\dot{V}_3 &= \dot{V}_2 + z_3 \dot{z}_3 \\
\dot{V}_3 &= -c_{11}z_1^2 - c_{12}z_2^2 - b_1 z_2 z_3 + z_3 \dot{z}_3 \\
\dot{V}_3 &= -c_{11}z_1^2 - c_{12}z_2^2 - b_1 z_2 z_3 + z_3(a_2(z_2 + \alpha_1) - a_2 u_a - \dot{\alpha}_2) \\
\dot{V}_3 &= -c_{11}z_1^2 - c_{12}z_2^2 - b_1 z_2 z_3 + a_2 z_2 z_3 + a_2 \alpha_1 z_3 - a_2 u_a z_3 - \dot{\alpha}_2 z_3
\end{aligned} \tag{4.9}
$$

To ensure convergence behaviour of all system states, rate of change of above calculated energy function $\dot{V}_3$ has to be decreasing function, for all values of z_1 z_2 and z_3 states. So, to meet said objective, the actual control input u_a is designed by replacing $\dot{V}_3$ with $-c_{13}z_3^3$, in 4.9. Where, c_{13} is actual control gain, the value of this gain determine how fast trajectory of z_3 is converging. This procedure is presented below:

$$\begin{aligned} -c_{13}z_3^2 &= -b_1 z_2 z_3 + a_2 z_2 z_3 + a_2 \alpha_1 z_3 - a_2 u_a z_3 - \dot{\alpha_2} z_3 \\ -c_{13}z_3 &= -b_1 z_2 + a_2 z_2 + a_2 \alpha_1 - a_2 u_a - \dot{\alpha_2} \\ u_a &= \frac{c_{13}}{a_2} z_3 - \frac{b_1}{a_2} z_2 + z_2 + \alpha_1 - \frac{1}{a_2} \dot{\alpha_2} \end{aligned} \tag{4.10}$$

Now by substituting actual control u_a into 4.9; we get.

$$\dot{V_3} = -c_{11} z_1^2 - c_{12} z_2^2 - c_{13} z_3^2 \tag{4.11}$$

The equation 4.10 represents that all z_1, z_2 and z_3 states are converging towards zero.

4.2 Simulation Results

In this section, simulation results of adaptive backstepping based controller have been presented, using SIMULINK/MATLAB software. The aim was to regulate bottom hole pressure and to minimize the effect of heave motion, in MPD systems, irrespective of variation in the system parameters. Design requirements was to track bottom hole pressure at 218 *bar* and to minimize pressure oscillation, in the presence of heave motion and varying parameter a_1. This controller has been tested for different types of varying amplitude and shape of applied heave motion.

4.2.1 Sinusoidal heave motion with one meter amplitude

Figures 4.1-4.4 are representing heave motion, bottom-hole pressure, choke valve opening percentage and parameter-estimator, simultaneously. In steady state, choke valve has to open and close between 48 and 52 *percent*, to accommodate described heave motion along with regulating bottom hole pressure at 218 *bar*. With tiny 0.35 *bar* negligible undershoot in transient, bottom-hole pressure remained free of pressure oscillations. According to shown figure 4.4, $\hat{a_1}$ gradually reach at a_1; and in steady state, error between a_1 and $\hat{a_1}$ becomes zero. In transient, choke valve opens at its maximum value, for less than 1 second, because of large error between $\hat{a_1}$ and a_1. By changing controller and parameter-estimator gain r, we can minimize specified control action spike but at cost of bottom-hole pressure fluctuation.

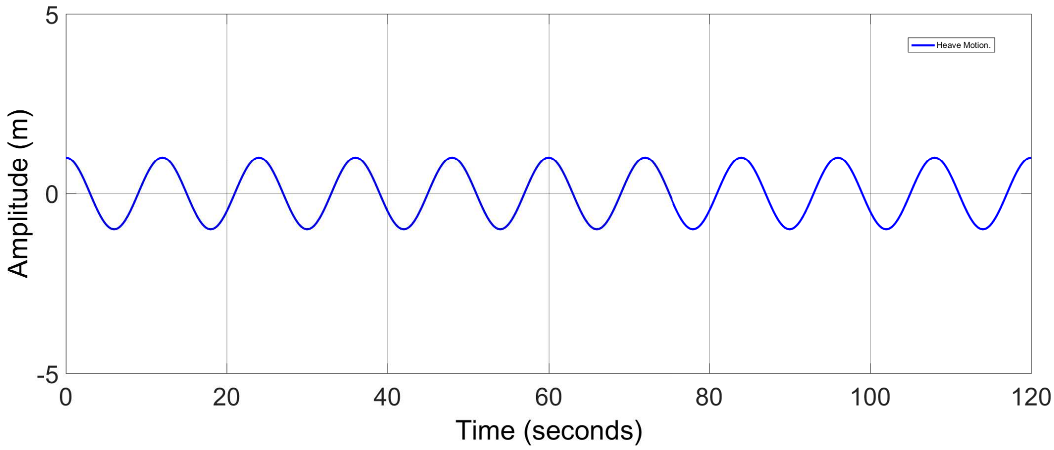

Figure 4.1: Heave Disturbance.

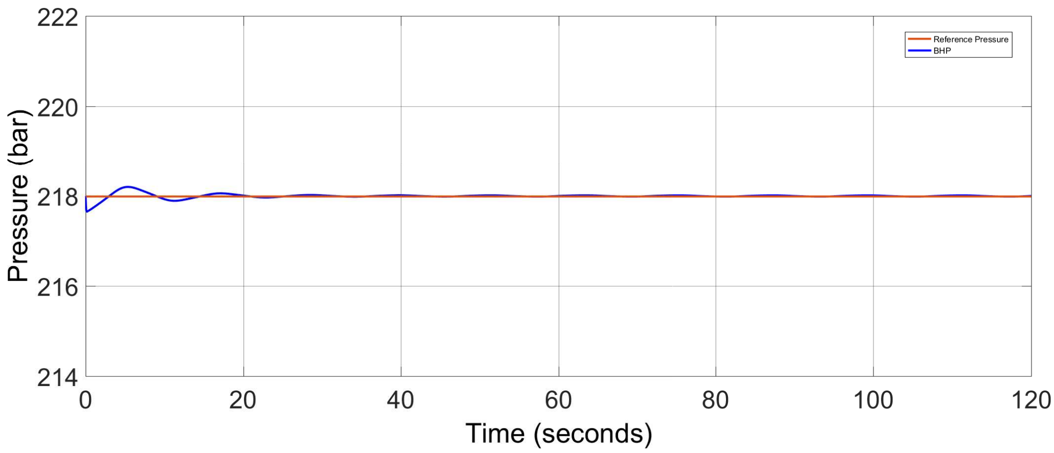

Figure 4.2: Bottom-hole Pressure.

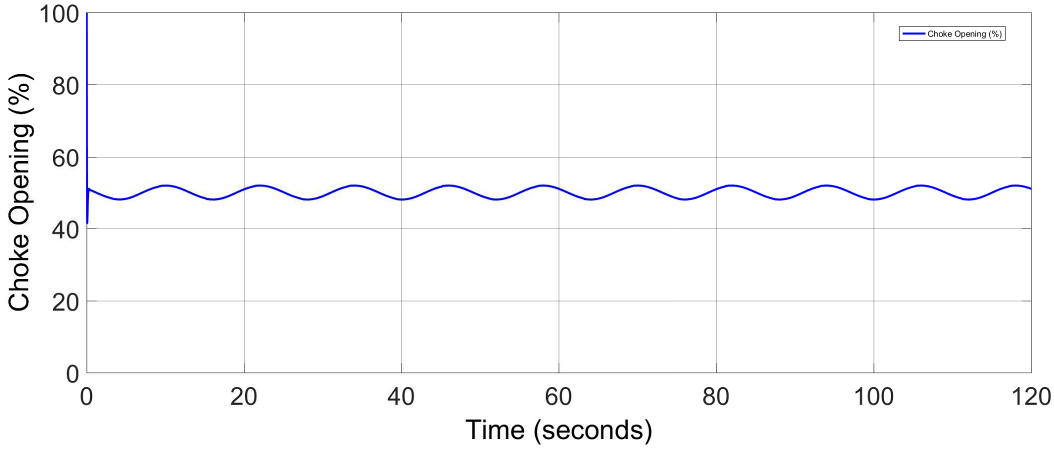

Figure 4.3: Choke Opening Percentage.

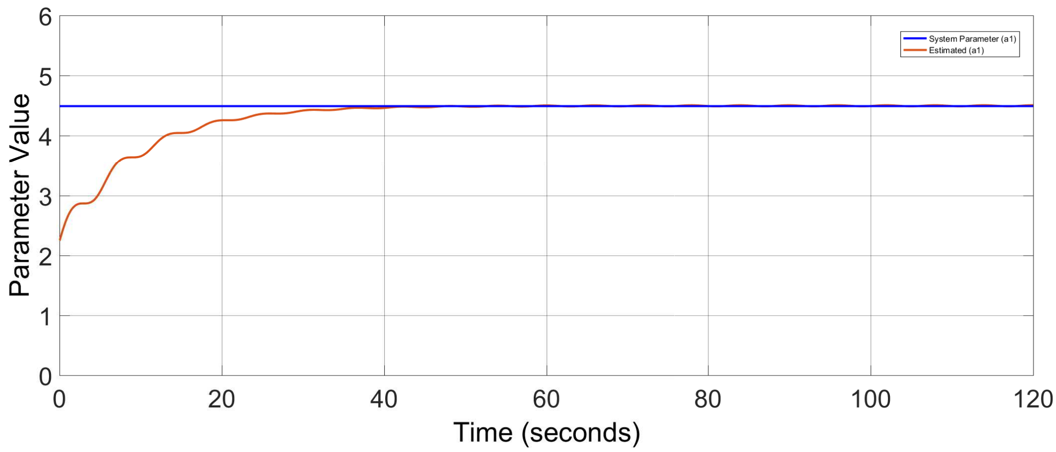

Figure 4.4: Estimation of a_1.

4.2.2 Sinusoidal heave motion with three meter amplitude

In [25], it is mentioned that the sea waves, having amplitude of 3 m, appears repeatedly, in North sea. As a result, to analyse the performance of proposed controller in more realistic way, heave motion having amplitude of 3 m has been used, in this simulation; and associated figures are from 4.5 to 4.8. In this scenario, choke valve opens and close a bit larger than previous case, above and below than its nominal value, 50 percent opening at equilibrium point, in steady state. Bottom hole pressure oscillations are still negligible, in decimal figure, but the value of undershoot is 1 *bar*. That is acceptable because maximum allowable window for pressure fluctuation in complex and deep sea is ± 2.5 *bar* [16]. The response of estimator is different than previous case as it includes small oscillations, in steady state. It is due to the effect of higher amplitude of heave motion. Initially, choke valve remained open at its maximum value, for almost $1s$, to compensate higher amplitude heave motion effect.

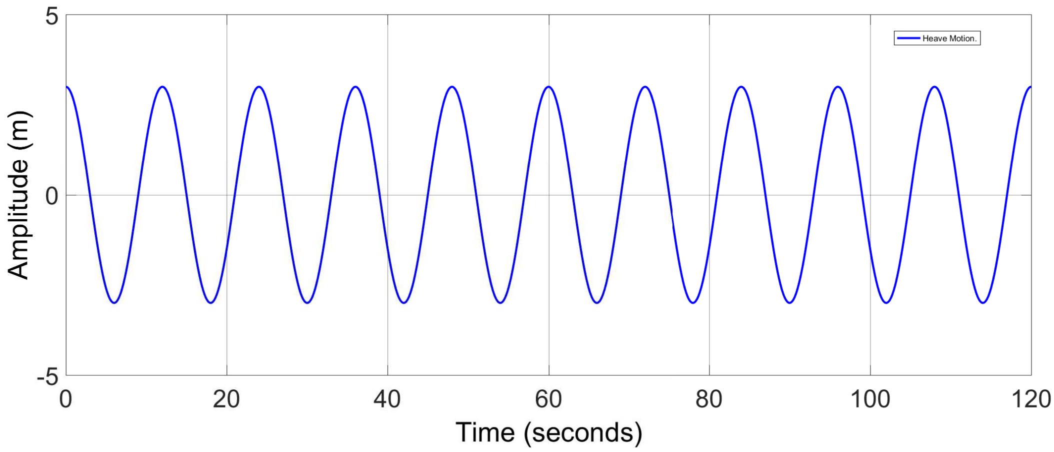

Figure 4.5: Heave Disturbance.

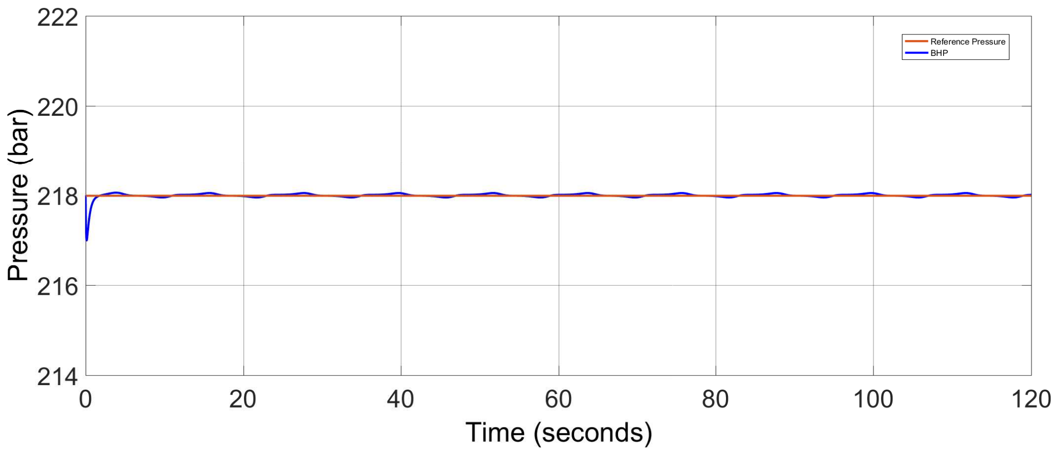

Figure 4.6: Bottom-hole Pressure.

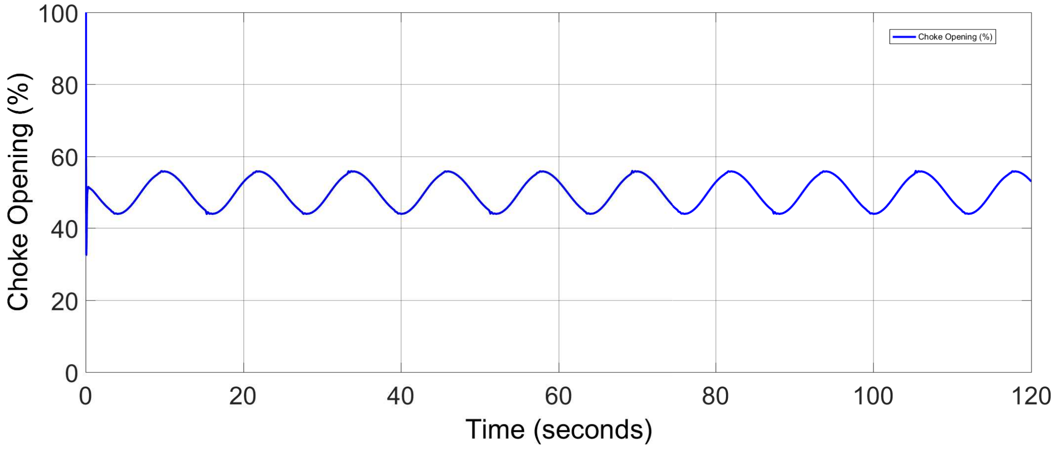

Figure 4.7: Choke Opening Percentage.

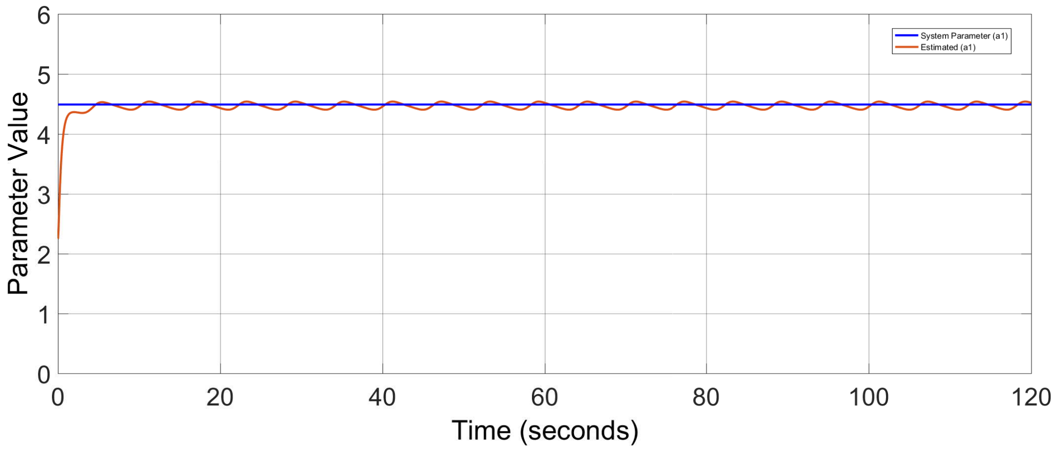

Figure 4.8: Estimation of a_1.

4.2.3 Sinusoidal heave motion with one meter sinusoidally varying amplitude

To analyse the effect of sea waves on managed pressure drilling process, in the presence of other waves already disturbing drilling process, heave motion model 2.9 is being used, in this simulation. With reference to figures from 4.9 to 4.16, all the results are almost similar to the results of subsection 4.2.1, except a slight difference in shape of oscillations. That is due to the shape of sinusoidally varying sinusoidal disturbance.

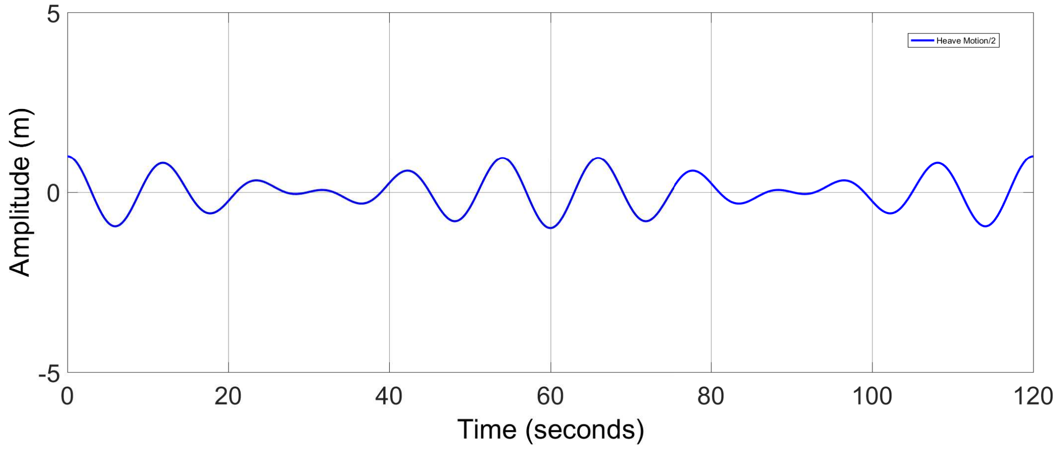

Figure 4.9: Heave Disturbance.

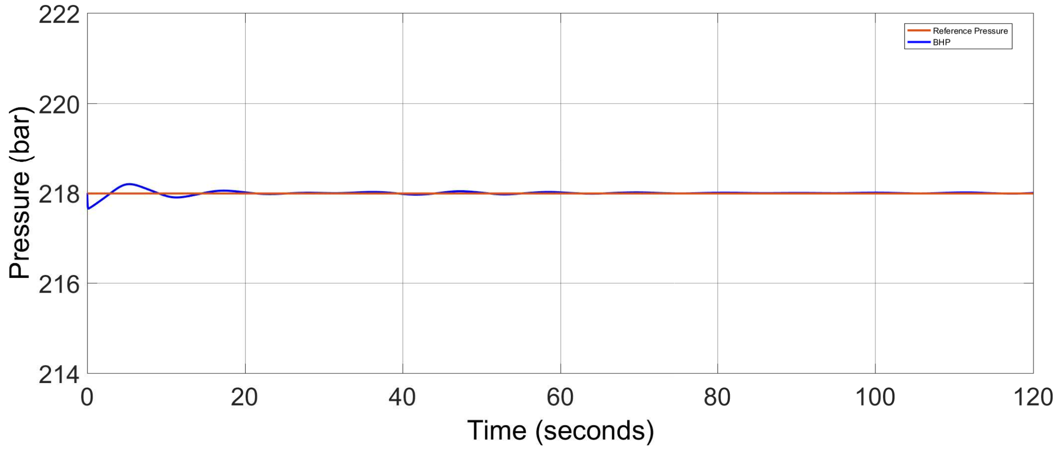

Figure 4.10: Bottom-hole Pressure.

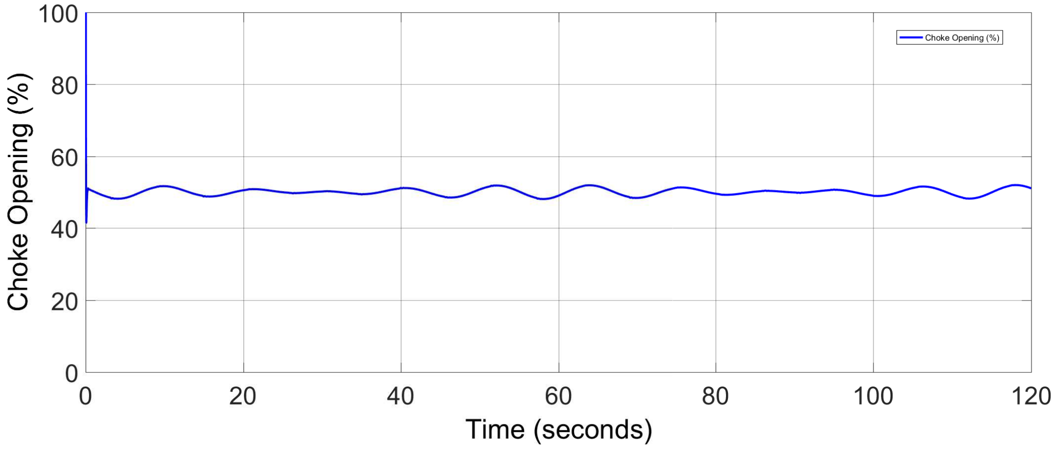

Figure 4.11: Choke Opening Percentage.

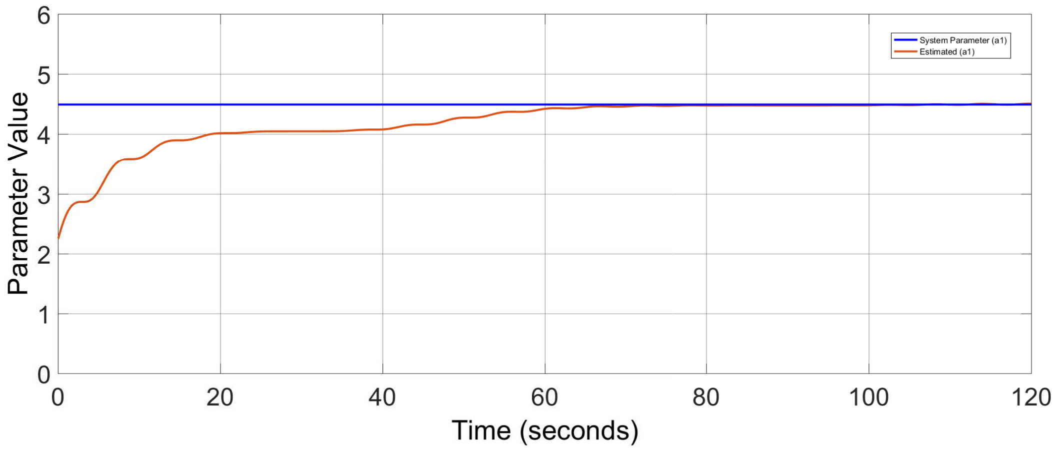

Figure 4.12: Estimation of a_1.

4.2.4 Sinusoidal heave motion with three meter sinusoidally varying amplitude

Using heave motion model described in 2.9, simulation results remained almost similar to 4.2.2 results. And again the shape is only changed due to changed shape of applied heave motion.

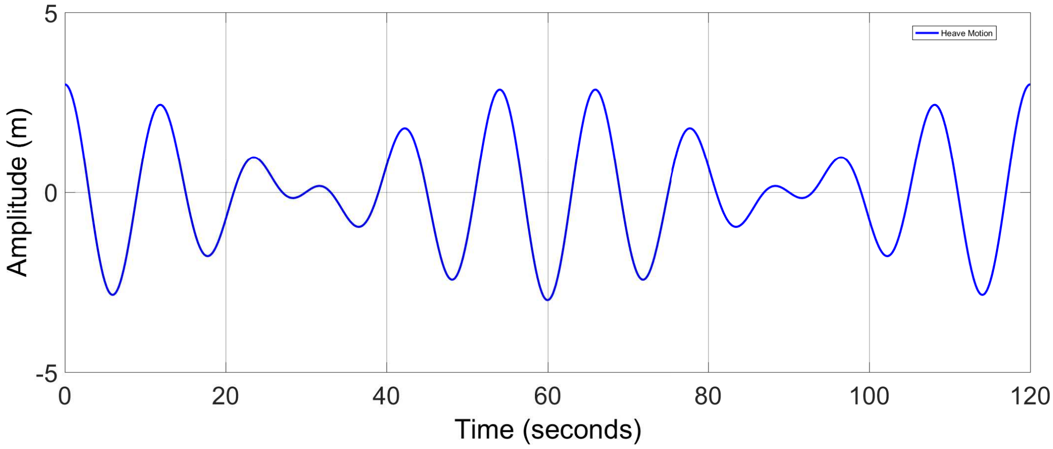

Figure 4.13: Heave Disturbance.

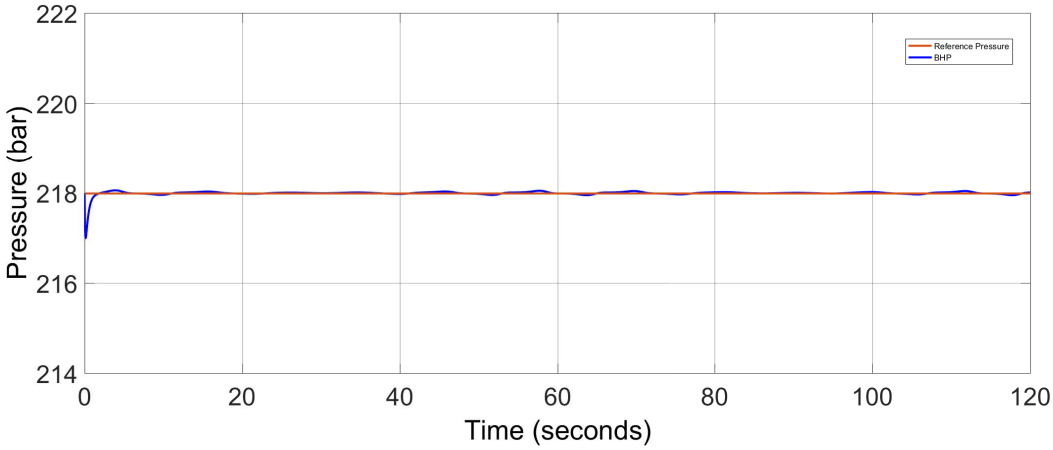

Figure 4.14: Bottom-hole Pressure.

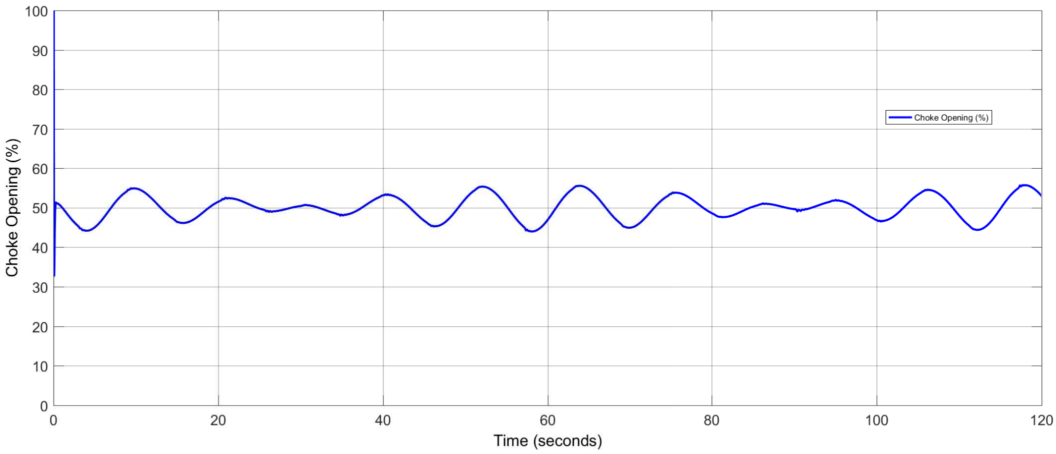

Figure 4.15: Choke Opening Percentage.

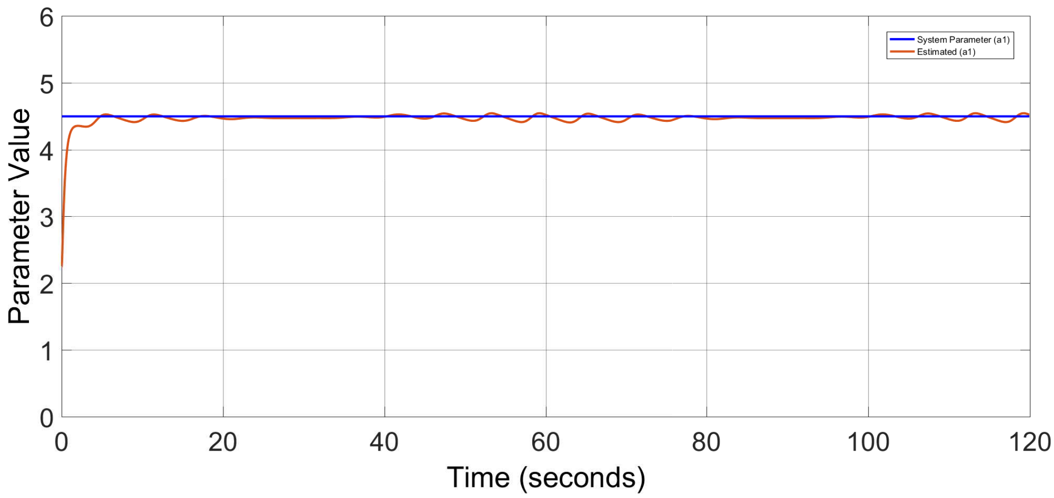

Figure 4.16: Estimation of a_1.

One important observation regarding discussed simulation results is that the gains of controller and estimator can be adjusted according to system requirements. Because these gain has direct relationship with system responses. If we increase the gains of controller or estimator, we can improve rise time and steady state response of the system but at cost of presence of overshot in transient response of the system. On the other hand, for smaller value of estimator and controller gains, we can dimmish overshoot from transient but system steady state response get distorted, due to presence of oscillation.

t

S.N	Control Type	BHP Oscillations in Steady State (*bar*)	Overshoot/ Undershoot
3	Internal Model Control	±1.80 *bar*	Very large
3	Output Regulation Control	±1.00 *bar*	Very large
4	Backstepping Control	±0.15 *bar*	No
5	Adaptive Backstepping Control	±0.04 *bar*	No

Table 4.1: Performance of Proposed Controllers.

In nutshell, one can adjust the gains of discussed controllers in different way, to achieve particular output response of the system.

4.3 Controller Performance

4.3.1 Oscillation suppression

As it is clear from results, adaptive backstepping controller achieved asymptotic rejection of heave disturbance. In the the presence of 1 m sinusoidal heave motion and varying a_1 parameter, controller worked efficiently well with negligible oscillations in bottom-hole pressure. Parameter estimator's performance is also commendable, it track system parameter accurately, shown in figure.

This section discusses performance of both controllers in term of their ability to suppress bottom-hole-pressure oscillations. Proposed controller's performance has been discussed with reference to other applied controllers, on same system, in the presence of ± 1 m heave disturbance. Set-point for bottom hole pressure is 218 bar. Ingar had proposed two controllers including output regulation controller and linear internal model controller for same system. These can be seen in [17], [24]. For comparison, Table 4.1 is presented.

4.3.2 Parameter Estimation

All the above discussed controllers, except adaptive backstepping controller, in table 4.1, are not capable to function properly for time varying system parameters. And almost every real dynamical system's parameters deviate from its nominal value, due to changing weather and model inaccuracy. Similarly, a_1 parameter in discussed managed pressure drilling system is assumed to be time varying. To cope with this time varying a_1 parameter, an adaptive backstepping controller is proposed. As it is evident from simulation results, it has performed efficiantly with fantastic accuracy. The estimator and controller both performed undoubtedly well, to suppress pressure oscillations and to estimate unknown parameter a_1.

Chapter 5

Conclusions and Future Work

5.1 Conclusion

Heave motion attenuation is an hot topic of research in MPD, hydrocarbon exploration industry. Because heave motion has severe impact on bottom-hole pressure oscillations; which leads to delaying in process and dangerous accidents etc. Since last decade, many researchers are trying to improve the efficiency of drilling process and they had proposed different controller for MPD. Their solution work properly but could only suppress pressure oscillation to some extent. The proposed backstepping controller is more effective in term of heave disturbance suppression, as it is evident form simulation results. In addition, the proposed adaptive backstepping controller has not only vanished pressure oscillations almost completely but it also has ability to deal with time-varying system parameter.

In a nutshell, these proposed controllers are more effective, reliable and safer for managed pressure drilling operations, for exploration of hydrocarbon.

5.2 Future work

A lot of future work can be suggested here;

- System parameters can be estimated to design robust control system for managed pressure drilling system.
- As pressure sensor does not work with accuracy in about more than 2 km deep sea, so nonlinear observer can be applied for state estimation.

- We can consider heave motion as a combination of sinusoidal waveforms having different frequencies and amplitudes to design more realistic control system.
- Analysis of proposed control systems can be performed in frequency domain, in order to do in dept analysis of effectiveness of the controllers.
- An optimum controller can be designed which can adjust online gains of designed controller for MPD. In this case, adaptive backstepping controller will perform excellently, irrespective of thousand percent of variation in parameters.
- Sliding mode controller can be applied on managed pressure drilling system.
- MPD model can be used for higher control volumes, to analyse its behavioue in more realistic manner.

Bibliography

[1] U. J. F. Aarsnes, "Modeling of two-phase flow for estimation and control of drilling operations," 2016.

[2] E. Hatlevik, "Heave disturbance attenuation in managed pressure drilling from a floating platform using model predictive control," 2014.

[3] F. Birol, "World energy outlook 2010," *International Energy Agency*, vol. 1, 2010.

[4] A. T. Bourgoyne, K. K. Millheim, M. E. Chenevert, and F. S. Young, "Applied drilling engineering," 1986.

[5] K. P. Malloy, R. Stone, G. H. Medley, D. M. Hannegan, O. D. Coker, D. Reitsma, H. M. Santos, J. I. Kinder, J. Eck-Olsen, J. W. McCaskill, *et al.*, "Managed-pressure drilling: What it is and what it is not," in *IADC/SPE Managed Pressure Drilling and Underbalanced Operations Conference & Exhibition*, Society of Petroleum Engineers, 2009.

[6] J. R. Smith, B. M. Patel, *et al.*, "A proposed method for planning the best initial response to kicks taken during managed-pressure-drilling operations," *SPE Drilling & Completion*, vol. 27, no. 02, pp. 194–203, 2012.

[7] O. Gabaldon, M. Culen, W. Bacon, P. Brand, *et al.*, "Enhancing well control through managed pressure drilling," in *Offshore Technology Conference*, Offshore Technology Conference, 2014.

[8] J. Eck-Olsen, P.-J. Pettersen, A. Ronneberg, K. S. Bjorkevoll, R. Rommetveit, *et al.*, "Managing pressures during underbalanced cementing by chok ing the return flow; innovative design and operational modeling as well as operational lessons," in *SPE/IADC Drilling Conference*, Society of Petroleum Engineers, 2005.

[9] J.-M. Godhavn *et al.*, "Control requirements for automatic managed pressure drilling system," *SPE Drilling & completion*, vol. 25, no. 03, pp. 336–345, 2010.

[10] O. N. Stamnes, J. Zhou, G.-O. Kaasa, and O. M. Aamo, "Adaptive observer design for the bottomhole pressure of a managed pressure drilling system," in *Decision and Control, 2008. CDC 2008. 47th IEEE Conference on*, pp. 2961–2966, IEEE, 2008.

[11] J. Zhou, O. Stamnes, O. Aamol, and G.-O. Kaasa, "Observer-based control of a managed pressure drilling system," in *2008 Chinese Control and Decision Conference*, pp. 3475–3480, IEEE, 2008.

[12] J. Zhou, O. N. Stamnes, O. M. Aamo, and G.-O. Kaasa, "Adaptive output feedback control of a managed pressure drilling system," in *Decision and Control, 2008. CDC 2008. 47th IEEE Conference on*, pp. 3008–3013, IEEE, 2008.

[13] J. Zhou, G. Nygaard, J.-M. Godhavn, Ø. Breyholtz, and E. H. Vefring, "Adaptive observer for kick detection and switched control for bottomhole pressure regulation and kick attenuation during managed pressure drilling," in *Proceedings of the 2010 American Control Conference*, pp. 3765–3770, IEEE, 2010.

[14] J.-M. Godhavn, A. Pavlov, G.-O. Kaasa, and N. L. Rolland, "Drilling seeking automatic control solutions," *IFAC Proceedings Volumes*, vol. 44, no. 1, pp. 10842–10850, 2011.

[15] Ø. Breyholtz, "Nonlinear model predictive pressure control during drilling operations," 2008.

[16] A. Nikoofard, T. A. Johansen, H. Mahdianfar, and A. Pavlov, "Design and comparison of constrained mpc with pid controller for heave disturbance attenuation in offshore managed pressure drilling systems," *Marine Technology Society Journal*, vol. 48, no. 2, pp. 90–103, 2014.

[17] I. S. Landet, A. Pavlov, and O. M. Aamo, "Modeling and control of heave-induced pressure fluctuations in managed pressure drilling," *IEEE Transactions on Control Systems Technology*, vol. 21, no. 4, pp. 1340–1351, 2013.

[18] H. Mahdianfar, N. Hovakimyan, A. Pavlov, and O. M. Aamo, "L 1 adaptive output regulator design with application to managed pressure drilling," *Journal of Process Control*, vol. 42, pp. 1–13, 2016.

[19] Ø. N. Stamnes, "Nonlinear estimation with applications to drilling," 2011.

[20] P. Skalle, *Pressure control during oil well drilling.* BookBoon, 2011.

[21] G.-O. Kaasa, "A simple dynamic model of drilling for control," *Statoil-Hydro Research Centre, Porsgrunn, Norway*, vol. 66, 2007.

[22] A. Pavlov, G.-O. Kaasa, and L. Imsland, "Experimental disturbance rejection on a full-scale drilling rig," *IFAC Proceedings Volumes*, vol. 43, no. 14, pp. 1338–1343, 2010.

[23] J. Zhou, Ø. N. Stamnes, O. M. Aamo, and G.-O. Kaasa, "Switched control for pressure regulation and kick attenuation in a managed pressure drilling system," *IEEE Transactions on Control Systems Technology*, vol. 19, no. 2, pp. 337–350, 2011.

[24] I. S. Landet, "Modeling and control for managed pressure drilling from floaters: Heave compensation by automatic nonlinear control," 2011.

[25] H. Mahdianfar and A. Pavlov, "Adaptive output regulation for offshore managed pressure drilling," *International Journal of Adaptive Control and Signal Processing*, 2016.